Efficient Forestation in the Brazilian Amazon: Evidence from a Dynamic Model*

Rafael Araujo† Francisco Costa‡ Marcelo Sant'Anna§

December 8, 2020

Abstract

This paper estimates the Brazilian Amazon's efficient forestation level. We propose a dynamic discrete choice model of land use and estimate it using a remote sensing panel with land use and stock of carbon of 5.7 billion pixels, at 30 meters resolution, between 2008 and 2017. We estimate that a business as usual scenario will generate an inefficient loss of 1,075,000 km^2 of forest cover in the long run, an area almost two times the size of France, implying the release of 44 billion tons of CO_2. We quantify the potential of carbon and cattle production taxes to mitigate inefficient deforestation. We find that relatively small carbon taxes can mitigate a substantial part of the inefficient forest loss and emissions, while only very large taxes on cattle production would achieve a similar effect.

JEL: *Q15, Q54, C35*

Keywords: *Dynamic Discrete Choice Model, Deforestation, Amazon, Land Use*

*We thank Torfinn Harding, Wolfram Schlenker, and seminar participants at AERE Summer Conference, GoSee, and FGV EPGE. Financial support is gratefully acknowledged from Rede de Pesquisa Aplicada FGV and from Coordenação de Aperfeiçoamento de Pessoal de Nível Superior - Brasil (CAPES) - Grant # 001.

†FGV EPGE and Climate Policy Initiative (e-mail: carlquist.rafael@gmail.com)

‡University of Delaware and FGV EPGE (e-mail: fcosta@udel.edu).

§FGV EPGE (e-mail: marcelo.santanna@fgv.br).

1 Introduction

Forest conservation is key to tackle climate change because of forests' capacity regulate the climate and store carbon (Bastin et al., 2019). Tropical forests hold an extraordinary amount of carbon. For instance, the Brazilian Amazon stored in 2000 the equivalent of more than 200 billion tons of CO_2, or the last 35 years of United States' fossil fuels emissions. Not surprisingly, deforestation is the main element responsible for CO_2 emissions in tropical ecosystems (IPCC, 2007). While preserving tropical forests has great social value for climate change and biodiversity, alternative uses of land can be economically valuable for the local population. Thus, whether completely halting deforestation is socially optimal is an empirical question.

In this paper, we estimate how far the Brazilian Amazon is from its efficient level of forest cover and stock of carbon. We then assess two policy approaches to get us closer to the Amazon's efficient stock of carbon in the steady state: a carbon tax based on the carbon content of the land and an *ad valorem* tax on the revenue from cattle ranching and agriculture. To do so, we propose and estimate a dynamic discrete choice model of land use where profit-maximizing farmers choose the use of the land: keeping it as native or secondary vegetation; using it as pasture grazing; or using it for growing cash crops. Land conversion is costly, which makes the farmers problem essentially dynamic and forward looking. We estimate the model with a rich panel dataset that classifies the land use of more than 5.7 billion pixels – at 30 meters resolution – for each year from 2008 to 2017 in the Brazilian Amazon (MapBiomas, 2019).

A growing literature studies land use decisions using static general equilibrium environments (*e.g.,* Costinot et al., 2016; Donaldson and Hornbeck, 2016; Pellegrina, 2020). Nevertheless, in order to study general equilibrium effects in an tractable framework, these models abstract from forward looking behavior and lumpy adjustments. A similar point can be made about the large literature that estimates the treatment effects of different policies used to mitigate deforestation (e.g. Alix-Garcia et al., 2015; Assunção et al., 2015; Jayachandran et al., 2017) and about discrete choice approaches that capture dynamic incentives using a reduced form (*e.g.,* Heilmayr et al., 2020; Lubowski et al., 2006, 2008).

In the context of land use in the Amazon, not only forest clearing involves private adjustment costs but also imposes a lumpy negative externality through the release of the stock of carbon accumulated in the forest. Thus, in order to estimate the long-run optimal forestation in the Amazon, and to understand how policies can shape the long-run stock of carbon in the forest, one needs a model that accounts for both the dynamic costly adjustments of land use and the option value of preserving the carbon stored in the land. The main contribution

of the paper is to propose and estimate such a model for the Brazilian Amazon.

We derive a model-based regression that allows us to recover the model structural parameters based on the transition probabilities of land use (as Scott, 2018). An advantage of our method is that it does not require strong assumptions on how agents make expectations about future prices and market conditions. The structural regression depends, essentially, on land use decisions based on the profit flows for each possible land use and the carbon stored in the land. A second advantage of our paper is the use of high-resolution data on carbon stock (Baccini et al., 2012) to investigate the relation between deforestation and the release of carbon at the pixel level granularity. By computing the tradeoff conservation versus economic rents for each plot of forest, we can map the exact areas that should be preserved but are under greater threat of being deforested.

We obtain the empirical analogs of the model from land use remote sensing data together with pixel level data of land suitability for crops and pasture, the amount of carbon stored in the forest, and transportation cost. To model return of crops, we combine potential yield for each crop, including pasture grazing, from the Food and Agriculture Organization's (FAO) project Global-Agroecologial Zones (FAO-GAEZ) with local prices data of agricultural products, and newly computed transportation cost.[1] Finally, we let the amount of carbon in the forest affect farmers decisions about conservation through a private "forest return," capturing some of the effects imposed by Brazilian environmental laws and command and control policies.

We estimate farmers' perceived value of carbon stored in the forest at \$7.26 per ton of CO_2. This is the value that rationalizes farmers' land use decisions in our sample. This suggests that environmental regulation in the Brazilian Amazon helps farmers to partially internalize the social value of the forest. However, famers' perceived value of carbon falls short of recent estimates of optimal carbon price, centered around \$50 per ton (EPA, 2016).

By combining our results of the perceived carbon value and the sensitivity of cropland, pastureland, and forest cover to this carbon value, we estimate that to achieve the efficient forestation imposed by a social cost of carbon of \$50 per ton, the Brazilian Amazon would be short 1,075,000 km^2 of forest cover to its optimal forestation level on the steady state – this is approximately two times the deforestation between 2001 and 2019. Importantly, on the steady state, the efficient forestation level would imply 44 billion tons of CO_2 not released into the atmosphere. This total amount of carbon saved is approximately equivalent to eight

[1] We estimate transportation costs in two steps as Donaldson (2018). First, we build a complete transportation network of Brazil using georefenced data on federal and states roads, ports, and waterways. Second, we fit a non-linear least squares model. With the results of this procedure we compute the transportation cost of each crop from any pixel in the Brazilian Amazon to international markets.

times U.S. emissions of fossil fuels in 2018 (Friedlingstein et al., 2019), or twice the CO_2 emissions from land use change in Brazil in the last twenty years(De Azevedo et al., 2018).

We then consider two policy counterfactuals to help the Amazon preserve the efficient amount of carbon in its forests. We first calculate how a carbon tax based on the carbon content of the land could shape farmers' incentive to deforest. We find that farmers' response to a carbon tax is convex. A carbon tax of US$10/ton would implement 84% of the socially optimal carbon emission reduction relative to status-quo land use. Meanwhile, a carbon tax as low as US$2.5/ton would already help mitigate 34% of the inefficient emissions in the steady state. This convexity follows from being cheap to preserve carbon deep in the forest, as both carbon stock and transportation costs are high. However, as the marginal land being preserved comes closer to the agricultural frontier, it becomes increasingly costly to preserve carbon.

Alternatively, we consider an excise tax on cattle ranching or agriculture production. Our counterfactuals show that we would need a 65% tax on cattle ranching to induce the same reduction in emissions as a $10/ton carbon tax. Taxing crops has virtually no effect on forest cover or emissions, as this activity still occupies a relatively small share of this region. This highlights the humongous public policy effort needed to mitigate carbon emissions in this context, as only very large excise taxes on Amazonian economic activities could produce efficient land use.

This paper contributes to different strands of the literature. A large literature studies optimal policies to fight deforestation in the Amazon (Pattanayak et al., 2010; Souza-Rodrigues, 2019; Assunção et al., 2019). We use the model's structure to compute the efficient steady state forestation – forest cover area and tons of carbon stored – in the Brazilian Amazon in a dynamic setting, and we quantify the effectiveness of market-based policy (product taxation) relative to a carbon taxation.

An important methodological contribution is that by using granular data on carbon stock, we disentangle the loss of forest cover from CO_2 emissions, and show that both variables are not linearly related as usually assumed (Assunção et al., 2015). As noted in Assunção et al. (2019), targeting environmental policies in a situation where government budget is overstretched can be of great importance. Here, we present a microfounded model that allows us to target location specific policies at the pixel level according to the amount of carbon stored in the vegetation. This can be especially relevant to mitigate the effect of policies that are known to put pressure on deforestation in designated areas, such as infrastructure building (Asher et al., 2020; Assunção et al., 2020).

Finally, we also contribute to the literature discussing cropland responses to prices and

the economic environment (Scott, 2018; Fezzi and Bateman, 2011; Chomitz and Gray, 1999; Lubowski et al., 2006; Sant'Anna, 2020). Our model estimates allow us to understand how farmers' choices between preserving the forest or using it for agriculture or cattle grazing are affected by crop prices in the long run. We find a long-run cropland elasticity with respect to crop prices higher than Scott (2018) estimates for the United States, even though there is a strong substitution effect between pastureland and cropland. This highlights different land use dynamics of a consolidated developed agricultural region – such as the United States – from a developing agricultural frontier, such as the Brazilian Amazon. In fact, our results are consistent with the ones found by Sant'Anna (2020) when studying sugarcane expansion in Brazil, using different dataset and estimation methods.

The paper proceeds as follows. Section 2 presents our model and derives the regression we will estimate to recover the model's parameters. Section 3 describes the empirical background and presents the data used to estimate the model. Section 4 discusses the identification and shows the results of the model estimation. We present the counterfactual results in Section 5. We discuss the main caveats of our exercise and present some extensions in Section 6, and we give our concluding remarks in Section 7.

2 Model

We formulate a dynamic discrete choice model where every year a profit maximizing agent chooses how to use each plot of land. We allow for three different uses: land can either be preserved, used for livestock grazing or agriculture. The agent can convert between different land uses subject to conversion costs. Following steps similar to Scott (2018), we derive a set of equations that allow us to estimate the parameters of the model using standard linear regression techniques. This derivation is carried out using a general treatment for flow profits in each use. We close this section with a detailed discussion on how we model those flow profits given data constraints. We present some of the model derivations in the Appendix Section A.

2.1 Setup

The basic unit of decision in the model is a field, denoted by i. Fields are grouped in locations, denoted by m.[2] Each field i is run by a rational decision maker that chooses the

[2]In our application, a field corresponds to a 30m resolution pixel from satellite imagery, while a location stands for a coarser 1km grid where individual fields are grouped. This distinction is important because many variables are only available at this coarser 1km grid.

profit maximizing land use for the field. Decision makers can choose among three possible land uses. They can plant cash crops, use the land as pasture for cattle grazing or leave it unused, typically, covered by native vegetation. We name the choice of the decision maker $j \in \{crop,\ pasture,\ forest\} =: J$. This choice is repeated every year $t = 1, \ldots, T$.

Each land use choice generates a profit flow $\pi_m(j, w_t, \varepsilon_{imjt})$ in year t that depends on the land use choice j, the field location m, market level variables (*e.g.*, prices) w_t and choice and time specific shocks ε_{imjt}. We assume a separable structure for the profit function:

$$\pi_m(j, w_t, \varepsilon_{imjt}) = r_m(j, w_t) + \varepsilon_{imjt}. \tag{1}$$

This assumption will be natural in our context of land use and yearly crops. For exposition purposes, we delay a thorough discussion of $r_m(\cdot)$ to the end of this section.

Decision makers must pay a land conversion cost $\Phi(j, k)$, where $j \in J$ denotes the current land use and $k \in J$ denotes the previous period land use. For instance, $\Phi(pasture,\ forest)$ denotes the cost (benefit) from deforestation and conversion of the field to pasture.

Assumption 1 *The evolution of market state variables follows a Markov process and it is conditionally independent from field level information (decisions and characteristics) – i.e.,* $F_{w_{t+1}|w_t,\varepsilon_{imjt},j} = F_{w_{t+1}|w_t}$.

Assumption 1 implies that field level decisions and characteristics do not affect the evolution of market level variables. This is consistent with the idea that decision makers are price takers in competitive final products markets.

Assumption 2 *Field level unobservables (to the econometrician)* ε_{imjt} *are independent over time and choices conditional on field characteristics and market level state variables, with type-I extreme value distribution.*

Assumption 2 is standard in the dynamic discrete choice literature. Assumptions 1 and 2 allow us, under usual regularity conditions, to write the decision maker's dynamic land use choice problem with the Bellman's equation:

$$V_m(k, w_t, \varepsilon_{imt}) = \max_{j \in J} \left\{ \Phi(j, k) + r_m(j, w_t) + \varepsilon_{imjt} + \rho E\left[\bar{V}_m(j, w_{t+1}) | w_t \right] \right\}, \tag{2}$$

where $\bar{V}_m(j, w_t) := E_\varepsilon \left[V_m(j, w_t, \varepsilon_{imt}) \right]$ and ε_{imt} is the vector of ε_{imjt} shocks for each choice j. It is helpful to denote the non-random component of (2) as

$$v_m(j, k, w_t) = \Phi(j, k) + r_m(j, w_t) + \rho E\left[\bar{V}_m(j, w_{t+1}) | w_t \right]. \tag{3}$$

We can then re-write the decision maker's problem as

$$V_m(k, w_t, \varepsilon_{ijmt}) = \max_{j \in J} \{v_m(j, k, w_t) + \varepsilon_{ijmt}\}. \tag{4}$$

The distributional assumption of logit errors implies the following conditional choice probability:

$$p_m(j|k, w_t) = \frac{\exp(v_m(j, k, w_t))}{\sum_{j' \in J} \exp(v_m(j', k, w_t))}, \text{ for } k, j \in J. \tag{5}$$

This is the probability a field transitions from land use k to land use j at location m and time t. The formulation above yields the Hotz and Miller (1993) inversion:

$$\log\left(\frac{p_m(j|k, w_t)}{p_m(j'|k, w_t)}\right) = v_m(j, k, w_t) - v_m(j', k, w_t), \text{ for } k, j, j' \in J. \tag{6}$$

That is, the ratio of conditional choice probabilities of different alternatives is directly related to the difference between the non-random components of returns from these alternatives.

Assumption 3 $\Phi(j, j) = 0$ *for all* $j \in J$ *– i.e., there is no conversion cost if land is not converted.*

From equations (3) and (6), using Assumption 3, we can write the dynamic probability of land conversion as

$$\log\left(\frac{p_m(j|k, w_t)}{p_m(k|k, w_t)}\right) - \rho \log\left(\frac{p_m(j|k, w_{t+1})}{p_m(j|j, w_{t+1})}\right) = (1-\rho)\Phi(j, k) + r_m(j, w_t) - r_m(k, w_t) + \eta_m^V(j, w_t) - \eta_m^V(k, w_t), \text{ for } j, k \in J, \tag{7}$$

where $\eta_m^V(j, w_t) := \rho(E\left[\bar{V}_m(j, w_{t+1})|w_t\right] - \bar{V}_m(j, w_{t+1}))$ denotes the expectation error in continuation values (see Appendix A for details).

The flow of profits $r_m(\cdot)$ is a key element to be estimated, and we provide a detailed discussion of its specification in the next subsection. For now, we only require that $r_m(\cdot)$ is linear in unknown parameters with an additive unobservable (to the econometrician) aggregate shock:

$$r_m(j, w_t) = \bar{\alpha}_j + \alpha_j' R_j(x_m, w_t) + \xi_{jm}(w_t), \tag{8}$$

where $R_j(x_m, w_t)$ are observed regressors and $\bar{\alpha}_j$ is an intercept – we normalize $\bar{\alpha}_{forest} = 0$.[3]

[3]This normalization is inevitable in any discrete choice application. It has no implication for the counterfactuals considered.

Structural regression equation. Finally, we recover a regression equation by substituting (8) into (7). For each location m, at year t:

$$\log\left(\frac{p_m(j|k,w_t)}{p_m(k|k,w_t)}\right)-\rho\log\left(\frac{p_m(j|k,w_{t+1})}{p_m(j|j,w_{t+1})}\right)=(1-\rho)\Phi(j,k)+\alpha_j'R_j(x_m,w_t)-\alpha_k'R_k(x_m,w_t)+$$
$$\bar{\alpha}_j-\bar{\alpha}_k+\xi_{jm}(w_t)-\xi_{km}(w_t)+\eta_m^V(j,w_t)-\eta_m^V(k,w_t),\ \text{for } j,k\in J. \quad (9)$$

The left-hand side depends only on conditional choice probabilities that can be observed (estimated) directly from the data. On the right hand side, we have regressors $R_j(x_m,w_t)$ and $R_k(x_m,w_t)$, an structural error $\eta_m^V(j,w_t)-\eta_m^V(k,w_t)$, which is mean zero conditional on information at t, transition specific intercept terms, and the aggregate shocks $\xi_{jm}(w_t)$ and $\xi_{jm}(w_t)$.

We let the $\bar{\alpha}_j$ absorb choice specific components which are constant across locations and time. This implies $\xi_{jm}(w_t)$ is mean zero across locations and time. Because $\xi_{jm}(w_t)$ and $\bar{\alpha}_j$ always appear as a sum, this a true normalization and innocuous to any counterfactual we consider.

To disentangle conversion costs $\Phi(j,k)$ from $\bar{\alpha}_j$ and $\bar{\alpha}_k$, we need to assume a grounding condition.

Assumption 4 *The fixed conversion cost from crop or pasture to forest is zero – i.e.,* $\Phi(forest,\cdot)=0$.

The intuition of Assumption 4 is that the agent does not incur in costs when transitioning from pasture or crop to reforestation. In other words, we assume that if we observe regeneration of forest in our data set, we assume that the land was only left idle. This is a natural assumption in our setting because the extent of active reforestation in the Amazon is minimal.

2.2 Flow of profits

We now discuss our specification of flow profits $r_m(\cdot)$ in (1) for each choice of land use.

Crop. In our setting, agriculture gives us a natural structure of flow profits for the crop land use. All products produced in each parcel of land could be transported to destination markets and sold at market price. The net revenue from this operation is equal to

$$(p_{ct}-z_{cm})y_{mc}+\bar{\alpha}_{crop}+\xi_{crop,m}(w_t), \quad (10)$$

where y_{mc} is the expected yield of crop c in location m, p_{ct} is the output price in destination markets, z_{mc} is the transportation cost from location m to destination markets, and $\bar{\alpha}_{crop} + \xi_{crop,m}(w_t)$ is a fixed cost associated with the crop land use that absorbs costs with inputs, wages, and other unobserved factors that are allowed to vary across locations and time.

We do not observe which crop is produced in each parcel. Instead, we use a weighted average of crops produced in location m's region, and measure the revenue (net of transportation cost) using

$$\tilde{r}_{mt} = \sum_{c \in \mathcal{C}} s_{cm} \left(p_{ct} - z_{mc} \right) y_{mc}, \tag{11}$$

where s_{cm} is the share of crop c in location m. Thus, the net payoff for the $j = crop$ land use becomes:

$$r_m(crop, w_t) = \alpha_{crop} \tilde{r}_{mt} + \bar{\alpha}_{crop} + \xi_{crop,m}(w_t). \tag{12}$$

The variable $\tilde{r}_{mt}$ and its associated coefficient α_{crop} will be extremely important in our analysis. The variable $\tilde{r}_{mt}$ is the only regressor measured in monetary units (in our case, Brazilian reais). We use its coefficient, α_{crop}, to give a monetary value to our counterfactuals.[4]

Pasture. A full structural model for pasture and livestock grazing is challenging given the essentially dynamic nature of cattle raising (see, e.g., Rosen et al., 1994). Here, instead, we propose a minimum structure for pasture flow profits that keeps some of the insights from the agriculture flow profit in (12):

$$r_m(j, w_t) = \alpha^1_{j,t} y_{m,j} + \alpha^2_j d_m y_{m,j} + \bar{\alpha}_j + \xi_{j,m}(w_t) \text{ for } j = pasture, \tag{13}$$

where d_i is road distance to port and $y_{m,pasture}$ is a measure of pasture suitability. The returns of using the land for pasture depends on the interaction of suitability and prices, which are flexibly represented by a time-varying coefficient. Like agriculture products, the production of livestock grazing must be transported to a destination market. We model transportation costs of pastures' output allowing its coefficient to differ according to pasture suitability, a transportation cost structure that is reminiscent of the one used for agriculture. Overall, we impose less structure to pasture flow profits, being considerably more flexible than for agriculture.

[4] An alternative equivalent presentation of our model would have $\tilde{r}_{mt}$ without an associated coefficient (as it is already measured in reais), but would allow for a dispersion parameter in the distribution of the logit shock ε_{imjt}. When standardizing such model dividing all payoffs by the standard deviation of ε_{imjt}, the inverse of the standard deviation of ε_{imjt} would be the coefficient for $\tilde{r}_{mt}$. Thus, we can interpret α_{crop} as the inverse of the standard deviation of the logit shock ε_{imjt}.

Forest. Finally, we model the return of leaving a field in location m unused to depend on the carbon stock of native vegetation h_m, so for $j = forest$, we have:

$$r_m(forest, w_t) = \alpha_{forest} h_m + \xi_{forest,m}(w_t), \tag{14}$$

where h_m denotes the carbon stock in location m. This variable captures the net effect of costs and benefits of maintaining the pixel forested. On the cost side, higher levels of carbon stored indicates an area of dense forest which may be more costly to clean and more susceptible to encroachment, since the delimitation of property may be blurred and more costly to enforce, resulting in potential loss of property rights or other damages (see, e.g., Hornbeck, 2010). On the benefit side, preserving an area with high carbon stock may be correlated with benefits such as protecting riparian forests and other sensitive areas, that could generate a direct benefit to farmers as well as avoid attention from enforcement authorities and avoid larger fines from not complying with environmental protection laws.

3 Background and Data

We use our model to investigate land use in the Brazilian Amazon. In this section, we provide a brief discussion about the state of land use and environmental regulation in the Brazilian Amazon and the data we use to estimate our model.

3.1 Land use in the Brazilian Amazon

We study land use in the Legal Amazon territory, the administrative region that includes the Amazon biome and that is subject to specific environmental and land use regulation. This region, depicted in Figure 1, covers more than five million squared km (61% of Brazilian territory). In 2000, forest covered 84% of the Legal Amazon area. After years of peak deforestation, the Brazilian government implemented a series of new environmental legislations and strengthened enforcement capacity between 2004 and 2007. Among other policies, the government created new protected areas (indigenous land and conservation units) and toughened the penalties for environmental crimes inside protected areas. The conservation policies implemented in this period were very effective to reduce deforestation in the following decade (Assunção et al., 2015; Burgess et al., 2019). We thus study the period between 2008 and 2017 when the Legal Amazon was under this new regulatory framework. Because land inside protected areas are subject to specific regulation (the green area in the map on the right of Figure 1), we exclude these areas from our sample.

Figure 1: Legal Amazon excluding Protected Areas (in green)

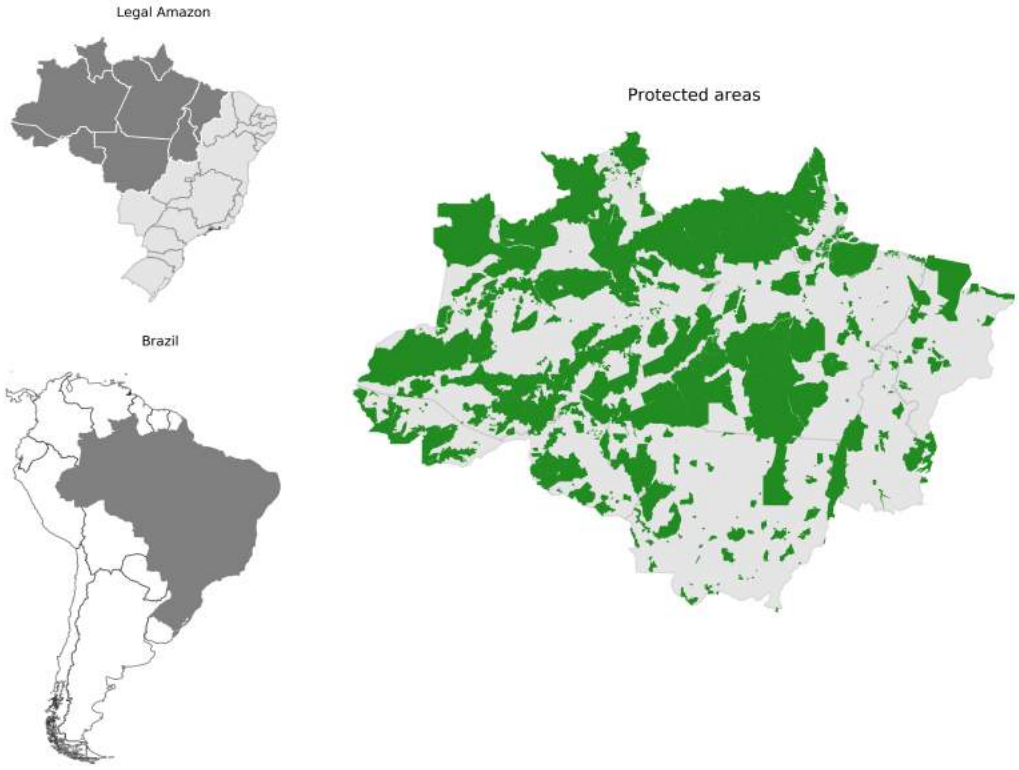

The figure shows the Legal Amazon territory and the Brazilian states. Our sample consists of the Legal Amazon area excluding the protected areas marked in green.

We obtain information on how each plot of land in the Amazon is used in this period from MapBiomas.[5] This data classifies the use of each pixel of 30m resolution in Brazil into several land use categories on a yearly basis. We aggregate land use into four categories: crops, pasture, forest, and others (in which we include non-classified pixels, urban areas, and water). This data shows that the main driver of loss of forest cover in the region has been the expansion of pasture for cattle ranching. In 2008, the area could be divided in 72% forest, 21% pasture, and 2% agriculture. Table 1 shows the share of forest, crop and pasture inside and outside protected areas in 2008 and 2017. We see that more than 93% of all crop and pastureland is outside protected areas.

[5]Project MapBiomas - Collection 4.0 of Brazilian Land Cover & Use Map Series, accessed on 20/01/2020 through the link: `http://mapbiomas.org`.

Table 1: Land Use Inside and Outside Protected Areas

	2008		2017	
	Non-protected	Protected	Non-protected	Protected
	(1)	(2)	(3)	(4)
Forest	0.49	0.51	0.48	0.52
Crop	0.98	0.02	0.97	0.03
Pasture	0.93	0.07	0.93	0.07
No data	0.72	0.28	0.73	0.27

This table shows for each land use the fraction of pixels inside protected areas and non-protected areas in 2008 and 2017. In each row, columns 2 and 3 and columns 5 and 6 add to 1.

3.2 Land use transition probabilities

The key information that we need to estimate our model are the transitions of each plot of land across different uses over the years. Table 2 illustrates the transition dynamics of all the pixels in the Legal Amazon outside of protected areas between 2008 and 2017. Each cell in the table indicates the probability of converting from land use 'row' in 2008 to land use 'column' in 2017. We observe that 4% of forest area in 2008 was converted to other uses in 2017, most of it to pasture. We see that 7.6% of cropland in 2008 converted to pastureland in 2017, and that 5.2% of pastureland in 2008 converted to cropland in 2017. At the same time, we see about 14% of pasture areas and 3.5% of cropland in 2008 going back to forest as secondary vegetation in 2017.

Table 2: Land Use Transitions in the Legal Amazon

	Forest	Crop in 2017	Pasture
	(1)	(2)	(3)
Forest in 2008	0.960	0.004	0.036
Crop in 2008	0.035	0.890	0.076
Pasture in 2008	0.140	0.052	0.800

Each cell indicates the probability of transitioning from land use 'row' in 2008 to land use 'column' in 2017. Rows do not add up to one because we omit the 'other' category – i.e., non-classified pixels, urban areas, and water.

Table 2 shows one of the main challenges in estimating our model: low transition rates in land use. Transition rate tends to be highly spatially correlated, with areas of dense forest composed of pixels that never face any transition over the ten years in our sample. This poses some challenges to our estimation, and we must take a few steps to go from the raw

land use data to the dependent variable needed to estimate the model.

Our key element to build the dependent variable in our regression equation (9) is the conditional choice probability $p_m(j|k, w_t)$ – that is, the probability of transitioning from land use k to j conditional on location and time. Our approach requires this conditional probability to be estimated non-parametrically. Even in a sample as big as ours, the curse of dimensionality in field characteristics implies that a full standard non-parametric attempt at estimating these conditional probabilities would be imprecise. Here, we follow Scott (2018) by computing the conditional probability to the two geographical dimensions: latitude and longitude. This reduces the number of field characteristic dimensions being used. We believe this is a good compromise for land use applications because all field characteristic variables vary smoothly over space, as we will show when we describe the rest of the data.

We depart from Scott (2018) on how we smooth over space when computing the transition probabilities. For a given pair of years (e.g., 2008 and 2009) and a transition (e.g., crop to pasture), we build a matrix of zeros and ones, where one indicates that a 30-meters pixel made this transition between those years. Because of the low transition depicted in Table 2, this matrix has many zeros. We then take the average of the nearby pixels reducing our dataset resolution from 30 meters to 1 km.[6] In addition, land use decisions are highly correlated across space, so working with a coarser resolution attenuates efficiency issues arising from this spatial correlation.

We can map this aggregation step directly into our model. The interpretation is that a 30-meters pixel represents a field – denoted by i in our model – and a 1-km pixel represents location – denoted by m – where our suitability measures $(y_{mc}, y_{m,pasture})$, transportation variables (z_{mc}, d_m), carbon stock (h_m) and most important the aggregate shocks $\xi_{j,m}(w_t)$ are homogeneous. This aggregation will be natural in our setting, given the resolution of the remaining variables explained in the next sections.

Even at 1 km resolution pixels, we still get many locations with close to zero transition rates. Those extreme conditional choice probabilities make it impossible to compute the Hotz-Miller inversion needed for model estimation. To deal with this, we smooth the probabilities of each location m by applying a Gaussian filter to the grid of locations.[7] This is a technique commonly used for image processing to blur images and reduce noise. With the conditional choice probabilities in hand, we compute the dependent variable of (9), taken as given the discount rate ρ.

[6] We reduce the resolution of the data also for computational reasons.

[7] We set the standard error of the Gaussian distribution to 150km. This value was chosen so that most of values averaged lies inside an area that is smaller than the average size of a state. When applying this filter, we ignore the transition coming from pixels inside protected areas.

3.3 Field characteristics

As detailed in Section 2.2, we use different land characteristics to model the land profitability under different uses in equations (12) to (14).

Potential crop returns. We model the return for crops specified in equation (12). That is, the return of crop in a field in location m in year t is the weighted average of the expected revenue from different common crops in location m's region, net of transportation costs to the nearest port. We consider soy and maize as possible crops, which constitute the bulk of cash crops produced in the Amazon. The weighting of these different crops taken by the share of each crop in m's mesoregion.[8] The share of each crop comes from the 2006 Census of Agriculture sourced by the Brazilian Institute of Geography and Statistics (IBGE).

Potential yield for each crop is from the Food and Agriculture Organization's (FAO) project Global-Agroecologial Zones, which gives estimation of crop-by-crop yields in kilograms per hectare at approximately 10km resolution. Those potential yields are given for a variety of scenarios, differing according to quantity of available inputs and water source. We use the yields of high inputs, which FAO describes as the market-oriented agriculture production, and rainfed cultivation, because this is the predominant form of production in the Brazilian Amazon. Figure 2 illustrates the potential yields for maize and soy in the region. We see that there is substantial variation in soy suitability, although the East and Southwest regions are more suitable for maize.

Last, to calculate the revenues of the potential yield, we use yearly maize and soy prices from the economic research center at College of Agriculture Luiz de Queiroz (ESALQ).

Potential pasture returns. We model the location-specific return for pasture grazing by interacting potential pasture suitability with year dummies and the transportation costs to the nearest port, as in equation (13). We use the potential suitability index for livestock grazing from FAO illustrated in Figure 2. Differently from our potential yield measures for soy and maize, the pasture suitability index is not measured in units of output per hectare. Given the flexible way we use this index in our pasture return specification (13), we believe this is not a serious limitation to our approach.

Carbon stock. We model the return of leaving the field i unused to depend on the carbon stock of native vegetation – equation (14). Our carbon stock data comes from the Woods

[8] A mesoregion is a classification from the Brazilian Institute of Geography and Statistics (IBGE) that groups contiguous municipalities with common geographic and social economic characteristics.

Figure 2: Agricultural and Pasture Potential Yield

(a) Maize

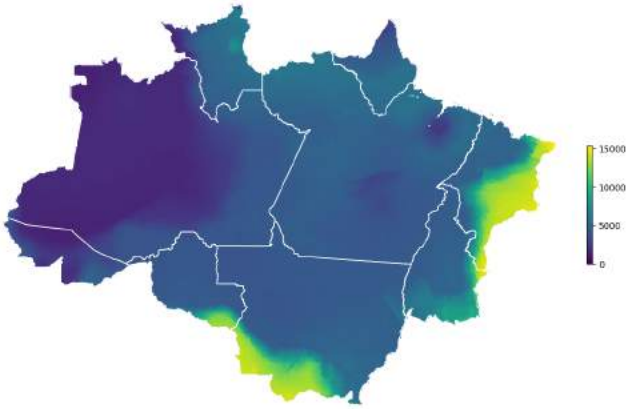

(b) Soy

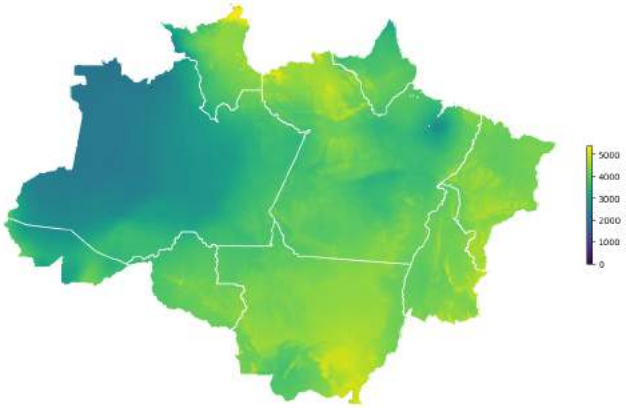

(c) Pasture

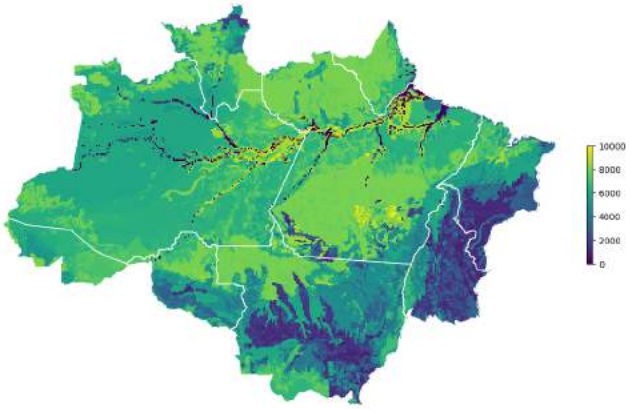

This figure plots the potential yield (kg per hectare) of maize (a) and soy (b), and the index for pasture suitability (c) from FAO-GAEZ. Values vary from blue (lower) to yellow (higher).

Hole Research Center, which provides values for 30m resolution of aboveground live woody biomass that we convert to potential of CO_2 release.[9] For exposition purposes we will call this measure the carbon stock.[10] This data is also key for our main counterfactual exercises, as it gives us a measure of location-specific social cost of deforestation, that is, the carbon in that pixel that will be released once deforested. Figure 3 shows the amount of carbon stock stored in the forest in 2000, the first year for which we have carbon stock data. One should expect that the carbon stored in areas that have been deforested to be smaller than the potential carbon that this same area could store once left idle for a long period of time. Because of that, we restrict our sample to pixels outside protected areas that were not deforested before the year 2000.

Figure 3: Carbon Stock in 2000

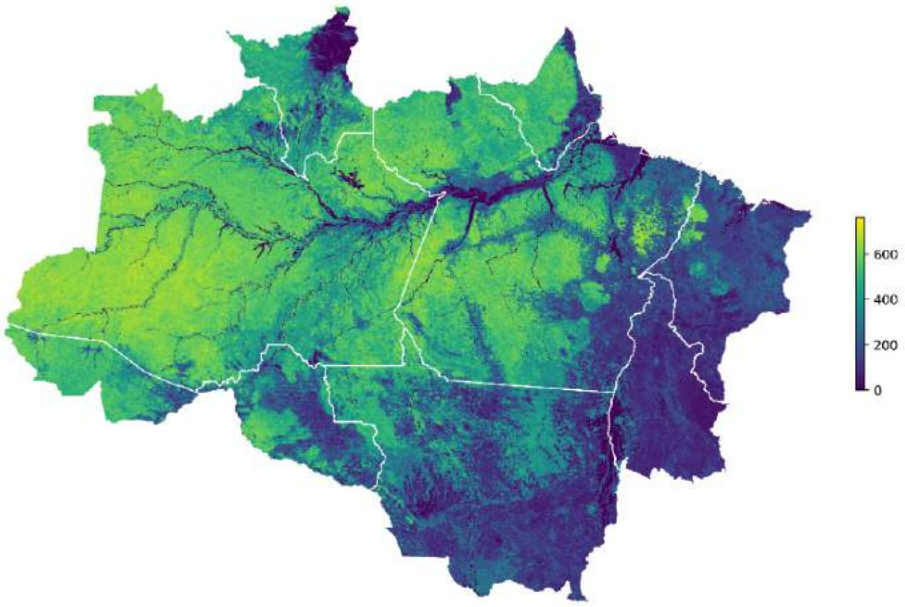

This map plots carbon stock density at 30m resolution. The values vary from blue (less carbon) to yellow (more carbon).

[9]We only consider aboveground biomass because: (i) it comprises most of the biomass (about a fifth of the biomass of tropical forests are below ground, IPCC, 2019); (ii) we have no granular data for belowground biomass; and (iii) most types of forest clearing do not release the belowground biomass into the air (Malhi et al., 2008)

[10]This dataset builds on the methodology of Baccini et al. (2012). The unit of measure in the original data is Mg Biomass per hectare. To convert biomass to CO_2 per hectare, this value must be divided by 2 – giving a measure of carbon (C) – and then multiplied by 44/12 – giving a measure of carbon dioxide (CO_2). Accessed through Global Forest Watch Climate on 02/04/2020. `https://data.globalforestwatch.org/datasets/aboveground-live-woody-biomass-density`.

3.3.1 Transportation costs

In our model, the decision maker chooses how to use the land considering the potential returns of crop and pasture net of transportation costs. To obtain that, we build the cost of transporting agriculture products from each pixel to the nearest export port. While the literature calibrates these parameters, we use a state-of-the-art data driven approach. This requires several steps and data sources, which we detail next.

Data on road networks and freight costs. First, we collect georeferenced data on federal and states roads from the National Bureau of Infrastructure DNIT.[11] The dataset informs whether each road is paved or unpaved, as shown in Figure A1. We convert this road network to our 1-km grid of locations and assign for each type of road a value that represents the cost to traverse that pixel. An important step is to estimate the cost of transporting agricultural commodities on paved and unpaved roads. We estimate the cost of traversing each type of pixel based on the internal freight costs collected by the Group of Research and Extension in Agroindustrial Logistics of the College of Agriculture Luiz de Queiroz (ESALQ). This data contains the transportation costs per ton of each product (maize and soy) between multiple municipalities for the years 2008-2013. We keep only pairs of origin/destination municipalities that connect at least one of the states of the Legal Amazon.[12]

Transportation cost by land. Second, we estimate the transportation cost by land over pixels with paved and unpaved roads using a non-linear least square (NLSS) estimation as Donaldson (2018). To do so, we first set up a grid of possible values for the costs of traversing each type of road, which we denote θ. For each θ, we apply Dijkstra's shortest path algorithm to generate an estimated (non-monetary) cost of transiting products from origin m to destination n for all origin/destination pairs (m, n) in the ESALQ's data. Let $TransitCost_{m,n}(\theta)$ be the cost for each value of θ and pair m, n calculated in this process. Note that this measure has no monetary interpretation. We use ESALQ's freight cost to estimate the monetary transportation cost based on θ. For each θ, we regress the freight cost for each product and origin/destination pairs (m, n) on our non-monetary transit cost:

$$FreightCost_{m,n,c} = \beta_{0,c} + \beta_{1,c} TransitCost_{m,n}(\theta) + \epsilon_{m,n,c}, \tag{15}$$

[11] Visited on 11/18/2018, `http://www.dnit.gov.br/mapas-multimodais/shapefiles`.
[12] Figure A2 plots all origin/destination pairs we use.

where $FreightCost_{m,n,c}$ is the monetized freight cost of transportation of one ton of product c between municipalities i and j from the ESALQ's dataset. The least squares objective function will be naturally linear in $\beta_{0,c}$ and $\beta_{1,c}$, but non-linear in θ due to the Dijkstra's algorithm. We choose the set of parameters θ that delivers the highest average R-squared.

The estimates of the best fit model is described in Table A1. This gives us the relative costs of transporting each product by land in the whole region. This model sets the cost of traveling over pixels with paved roads equal to 1, unpaved road equal to 2, pixels with no state or federal roads equal to 5, and pixels without roads inside protected areas equal to 10. These values, especially for protected areas, seem low when compared with calibrated values from the literature (see, e.g., Souza-Rodrigues, 2019). Nonetheless, increasing the cost of travelling over pixels inside protected areas do not make much difference for the estimation because our estimated parameters are already high enough that agents avoid travelling by these pixels.

Transportation cost by water. Third, we calculate the transportation cost by waterways, a commonly used transportation mode in the Amazon. Differently from roads, we cannot quantify the transportation costs between all origin/destination pairs. Instead, we model waterway transportation as an expressway to reach international markets. To do so, we collected GIS data on all Brazilian ports and waterways from the Ministry of Transportation. We differentiate between two types of ports: (i) final ports in which goods can be directly shipped to the international market, those with easy access to the sea; and (ii) loading ports, used as entrance to the waterways. We set the cost to traverse a pixel with waterway equal to half the cost to traverse a paved road. Figure A3 shows the location of the main ports and the non-monetary cost to reach a final port for each loading port – final ports have zero costs.

Minimum shipping costs. In the last step, equipped with the transit costs by roads and by waterways, we compute the minimum cost to ship products from every location in our sample to the nearest final port, using Dijkstra's algorithm. We transform this transit cost to a monetary value using the estimated values from equation (15). We end up with a monetary cost to transport each product from each location to an international port. Figure 4 plots the transportation cost of soy.

Connecting to the model. We compute the transportation cost for soybeans and maize – $z_{m,soybeans}$ and $z_{m,maize}$ in the model. For the pasture variables, we use the non-monetary

cost – prior to the transformation to a monetary value via the linear regression – d_m in the model.[13]

Figure 4: Transportation Costs for Soy

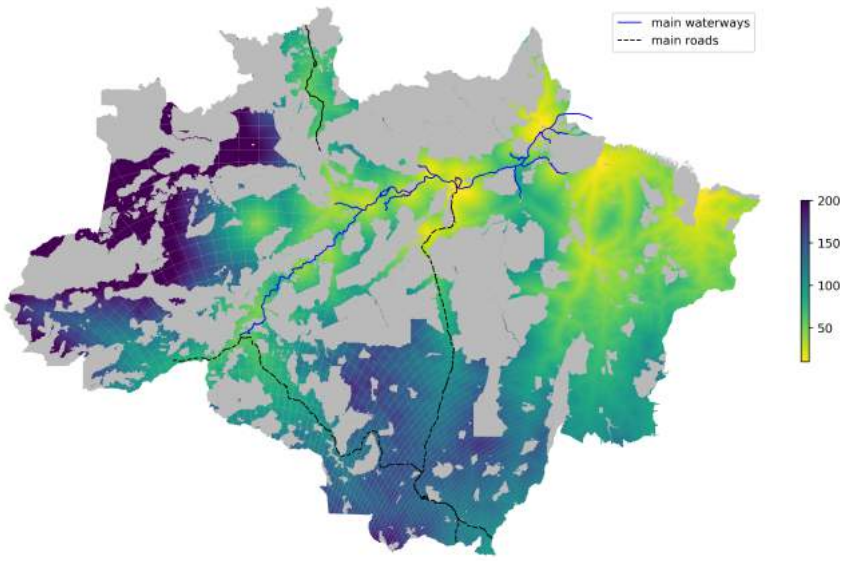

This map plots the minimum transportation costs of soybeans from every pixel to the international market in reais (R$) per ton. The values were capped at 200 for better visualization.

3.4 Summary statistics

We close this section presenting summary statistics for the main cross section variables used to estimate the model. Table 3 shows considerable cross-section variation in agricultural suitability and transportation costs. This variation is important because we are interested in performing counterfactuals with permanent price shifts. In our model, a permanent increase in prices is equivalent to an increase in agricultural potential yields or a decrease in transportation costs. Thus, the cross-section variation on the net returns of crop and livestock grazing is key to calculate price elasticities based on the model.

4 Identification and Estimation

We want to estimate the structural equation (9) which relates the conditional choice probabilities and the potential returns of the different land uses. We proceed in steps, first

[13]We do this because if we used the monetary cost for pasture instead, it would include another constant to the model: the regression constant.

Table 3: Descriptive Statistics

Variable:	Potential yield			Transportation cost		Carbon Stock
	Maize	Soy	Pasture	Maize	Soybean	
Model analog:	$y_{m,maize}$	$y_{m,soy}$	$y_{m,pasture}$	$z_{m,maize}$	$z_{m,soy}$	h_m
Unit:	(ton/ha)	(ton/ha)	(index)	(R$/ton)	(R$/ton)	(ton/ha)
	(1)	(2)	(3)	(4)	(5)	(6)
mean	5.61	3.32	5115.26	103.53	102.42	310.20
std	1.43	0.59	2252.12	61.22	62.09	239.50
min	0.00	0.00	0.00	7.79	5.32	0.00
25th percentile	5.12	3.10	3923.00	57.20	55.43	34.83
50th percentile	5.33	3.52	5611.00	93.01	91.75	330.00
75th percentile	5.66	3.72	6672.00	137.72	137.10	537.16
max	10.63	4.54	10000.00	571.58	577.13	856.16

This table shows descriptive statistics for the field characteristics used in the model's estimation. The second line of the column name points to the corresponding variable in the model. Transportation costs are in reais (R\$) from 2008, the first year we have data on transportation cost. The last column shows the carbon stock per hectare.

estimating the coefficient of returns of crop, then estimating the coefficients attached to carbon stock, pasture, and conversion costs.

Coefficient of crop. We want to allow for systematic differences across locations in the unobservables $\xi_{jm}(w_t)$. Therefore, we take differences over time in (9) to eliminate the fixed location specific component of $\xi_{jm}(w_t)$:

$$\Delta Y_{j,k,m,t} = \alpha_{crop} X_{j,k,m,t} + (\alpha^1_{pasture,t} - \alpha^1_{pasture,t-1}) W_{j,k,m,t} + \Delta\zeta_{j,k,m,t}, \tag{16}$$

where $X_{j,k,m,t}$ and $W_{j,k,m,t}$ are, respectively, the returns in difference for crop and pasture defined as:

$$X_{j,k,m,t} = \begin{cases} (\tilde{r}_{mt} - \tilde{r}_{m,t-1}) & \text{, if } j = crop \text{ and } k \neq crop, \\ -(\tilde{r}_{mt} - \tilde{r}_{m,t-1}) & \text{, if } k = crop \text{ and } j \neq crop, \\ 0 & \text{, otherwise.} \end{cases}$$

$$W_{j,k,m,t} = \begin{cases} y_{m,pasture} & \text{, if } j = pasture \text{ and } k \neq pasture, \\ -y_{m,pasture} & \text{, if } k = pasture \text{ and } j \neq pasture, \\ 0 & \text{, otherwise.} \end{cases}$$

Note that forest return is not in this equation because it does not vary across time. The dependent variable is also a first difference of the dependent variable of equation (9):

$$\begin{aligned}\Delta Y_{j,k,m,t} = &\left[\log\left(\frac{p_m(j|k,w_t)}{p_m(k|k,w_t)}\right) - \rho\log\left(\frac{p_m(j|k,w_{t+1})}{p_m(j|j,w_{t+1})}\right)\right] \\ &- \left[\log\left(\frac{p_m(j|k,w_{t-1})}{p_m(k|k,w_{t-1})}\right) - \rho\log\left(\frac{p_m(j|k,w_t)}{p_m(j|j,w_t)}\right)\right]\end{aligned}$$

Finally, the error term is:

$$\begin{aligned}\Delta\zeta_{j,k,m,t} = &\left[\eta_m^V(j,w_t) - \eta_m^V(k,w_t)\right] - \left[\eta_m^V(j,w_{t-1}) - \eta_m^V(k,w_{t-1})\right] \\ &+ \left[\xi_{j,m}(w_t) - \xi_{k,m}(w_t)\right] - \left[\xi_{j,m}(w_{t-1}) - \xi_{k,m}(w_{t-1})\right]\end{aligned}$$

This procedure, however, creates endogeneity in the regression (16) because the error term $\eta_m^V(j,w_{t-1})$ is a difference of expected and realized values, thus correlated with $\tilde{r}_{mt}$. To circumvent this identification issue, we follow Anderson and Hsiao (1981) and use lagged values of returns ($\tilde{r}_{m,t-2}$) as instrument for $X_{j,k,m,t}$.[14] This is a valid instrument since $\tilde{r}_{m,t-2}$ is information known at $t-1$, so uncorrelated with the expectational error $\eta_m^V(j,w_{t-1})$.

Table 4 presents the results of estimating equation (16). The third column displays our baseline estimates. As expected, we find that α_{crop} coefficient is positive, that is an increase in crop returns increase the likelihood of land being converted to crop. The results for the first stage, where we regress the returns variable in difference ($X_{j,k,m,t}$) on its lagged value in level ($\tilde{r}_{m,t-2}$) is presented in Table A2.

Coefficients of pasture and carbon stock. In a second step, we use the estimated $\hat{\alpha}_{crop}$ and $\Delta\alpha^1_{pasture,t}$ to estimate the remaining parameters in equation (9) by ordinary least squares. Table 5 shows the results. The variables composing the pasture return do not have a structural interpretation, since those variables are used to flexibly model the returns of livestock grazing.

The coefficient attached to the field's carbon stock, instead, has economic interpretation. The carbon stock variable has a positive coefficient, indicating that a higher stock of carbon in a plot of land decreases the likelihood of this plot being converted to other uses. By monetizing the carbon stock coefficient – *i.e.*, dividing it by α_{crop} –, we estimate that farmers' perceived value of preserving carbon in the forest is equal to R$ 1.50 per ton of CO_2 per

[14] We could, in principle, estimate the model using the Arellano and Bond (1991) estimator as Scott (2018). The difference of the two estimators is the asymptotic efficiency. Due to the size of our data set – we have 79,473,168 observations in our main specification –, efficiency is not a problem. Besides that, the size of our data set would make it difficult to implement this estimator.

Table 4: Crop flow profit coefficient

Regressor	Model Parameter	Estimate
$X_{j,k,m,t}$	α_{crop}	0.00039***
		(1.61e-6)
$W_{j,k,m,2011}$	$\Delta\alpha^1_{pasture,2011}$	3.46e-5***
		(8.04e-8)
$W_{j,k,m,2012}$	$\Delta\alpha^1_{pasture,2012}$	-9.93e-6***
		(4.53e-8)
$W_{j,k,m,2013}$	$\Delta\alpha^1_{pasture,2013}$	-4.01e-5***
		(6.55e-8)
$W_{j,k,m,2014}$	$\Delta\alpha^1_{pasture,2014}$	3.11e-5***
		(5.86e-8)
$W_{j,k,m,2015}$	$\Delta\alpha^1_{pasture,2015}$	-5.57e-5***
		(4.52e-8)
$W_{j,k,m,2016}$	$\Delta\alpha^1_{pasture,2016}$	5.87e-5***
		(8.89e-8)

This table shows the estimates of α_{crop} obtained in the second stage regression (equation 16) using Anderson and Hsiao (1981) estimator. The first column reports regressors, while the second column displays the corresponding model parameters from Section 2.2, equations (13) and (14). Robust standard errors in parenthesis. Number of observations 79,473,168.

year. Taking this annual benefit of preserving carbon stored at present value using a 5% interest rate, we estimate a perceived value of carbon of $ 7.26 per ton of CO_2.[15] This suggests that Brazilian environmental regulation makes farmers internalize at least part of the social value of the carbon stored in the forest. However, farmer's perceived value of carbon is substantially smaller than most estimates of the social value of carbon, starting at US$ 18.50/ton (Nordhaus, 2014) and centered around US$ 42/ton (EPA, 2016). That is, our estimates point that farmers, when choosing to deforest a plot of forest, do not take in consideration the full social costs of their action.

Transition costs. Finally, we also recover the conversion costs. As we explain in Section 3, we assume that converting pasture or cropland to forest has zero fixed cost, that is, forest regeneration happens through leaving the land idle. Under Assumption 4, we can recover the remaining parameters of the model: transitioning fixed cost, $\Phi(j,k)$, and the choice specific constants, $\bar{\alpha}_j$.

Table 5 shows the recovered parameters. The conversion costs are all internally consistent. We estimate that transition costs of clearing forest to grow crops is larger than clearing the

[15] We use the exchange rate of R$ 4.14 per USD $ from December 2019.

Table 5: Forest and pasture flow profits coefficients

Regressor	Model Parameter	Estimate	$\backslash\alpha_{crop}$
h_m	α_{forest}	0.00058***	1.50
		(4.12e-7)	
$W_{j,k,m}$	$\alpha^1_{pasture,2011}$	6.45e-5***	-
		(3.51e-8)	
$W_{j,k,m}d_m$	$\alpha^2_{pasture}$	-6.33e-7***	-
		(1.89e-9)	
Fixed effects			
	$\Phi(pasture, forest)$	-6.23e-1***	-1614.54
		(1.56e-4)	
	$\Phi(crop, forest)$	-9.68e-1***	-2511.25
		(2.95e-4)	
	$\Phi(crop, pasture)$	-5.97e-1***	-1574.21
		(3.04e-4)	
	$\Phi(pasture, crop)$	-2.00e-1***	-519.02
		(3.02e-4)	
	$\bar{\alpha}_{pasture}$	1.79e-1***	464.23
		(1.78e-4)	
	$\bar{\alpha}_{crop}$	-5.87e-1***	-1523.52
		(2.49e-4)	

This table presents the OLS estimates of equation (9), using $\hat{\alpha}_{crop}$ and $\Delta\alpha^1_{pasture,t}$ estimated in equation (16) using Anderson and Hsiao (1981). The first column reports regressors, while the second column displays the corresponding model parameters from Section 2.2, equations (13) and (14). Robust standard errors in parenthesis. Number of observations: 79,473,168.

forest to create pasture. This is also intuitive as preparing the land for agriculture after clearing the forest requires more investments in the land (such as removing stumps, and leveling the terrain) than when preparing a pasture. Furthermore, the transition costs of clearing forest land to grow crops is close to the sum of the transition costs from forest to pasture and the transition from pasture to crop.

5 Counterfactuals

In this section, we use our estimated model to assess the efficient forest cover and to discuss alternative policies to mitigate inefficient emissions. In the language of discrete choice modeling, we calculate the counterfactual conditional choice probabilities (CCP) for the alternative scenarios and evaluate their implications for outcomes of interest. The value function for each alternative scenario is the key ingredient that needs to be computed to

obtain the CCP's using (5).[16] This computation of the value function needs to be performed numerically and is slowed down by the size of the state space. We make an important simplification here: we remove all uncertainty about market state variables (w_t) in the model, that is, we assume they are constant in the counterfactuals. From equations (3) and (21), we iterate the following expression to obtain the value function of the recursive problem:

$$\bar{V}_m(k,w) = \log\left(\sum_{j\in J} \exp\left(\Phi(j,k) + r_m(j,w) + \rho\bar{V}_m(j,w)\right)\right) + \gamma. \tag{17}$$

In defining the return variable $r_m(j,w)$ we set the aggregate shock $\xi_{j,m}(w)$ to zero. With $\bar{V}_m(j,w)$ computed, we use expressions (3) and (5) to compute the CCPs. We then compute the invariant distribution of each location m, which gives a steady-state probability of one pixel in m being in a specific state. Aggregating for all locations, we obtain the steady-state land use, which we call $A^*(j,w)$. This object is the basis for our counterfactual exercises.

5.1 Long-run effects of higher agricultural prices

In our first counterfactual exercise, we assess how a variation in agricultural prices affects land use and carbon release. Although this counterfactual is only indirectly linked to our main research questions, it is of interest on its own and helps situate our results in the wider literature. Here, we compare the steady state land use $A^*(j,w)$ with and without the price change and compute a long-run elasticity of land use with respect to agricultural prices:

$$\partial_{j,\Delta} = \frac{A^*(j,w(1+\Delta)) - A^*(j,w)}{A^*(j,w)}\frac{1}{\Delta}. \tag{18}$$

Table 6 Panel A reports land use elasticities with respect to agricultural prices. We observe a high own land use price elasticity of 6.3 for cropland (column 2). Although this is high compared with evidence for the US reported in Scott (2018), it is in the ballpark of similar measures in the context of Brazilian agriculture, e.g., Sant'Anna (2020). We can also see that, although the conversion of pasture to crop is high (with an elasticity of -0.23), most of the cropland increase is over forest. Our model estimates an elasticity of forest cover with respect to agricultural prices of -0.45. These results are consistent with the literature arguing that market conditions increase the pressure from agriculture over forest land in areas where the agriculture frontier is non-consolidated,[17] as is common in countries with

[16] Note that estimation is performed without the need to solve for the value function. This is a convenient feature of the estimator proposed by Scott (2018), which is shared by many other commonly used dynamic discrete choice estimators (*e.g.,* Hotz and Miller, 1993; Aguirregabiria and Mira, 2007).

[17] E.g., Gibbs et al. (2015); Assunção et al. (2015); Souza-Rodrigues (2019); Harding et al. (2019).

tropical forests.

Table 6: Long-run land use elasticities with respect to prices

Forest Cover	Crop Area	Pasture Area	Carbon Released
(1)	(2)	(3)	(4)
Panel A. Crop price elasticities			
-0.45	6.3	-0.23	0.11
Panel B. Cattle price elasticities			
-1.64	-0.45	1.34	1.66

This table presents long-run elasticity of forest cover, crop area, pasture area and carbon released with respect to an crop price (*Panel A*) and with respect to cattle price (*Panel B*). Elasticities calculated with $\Delta = 0.1$ (eq. 18).

In the fourth column of Table 6, we use the granularity of our carbon data to compute the effects of the price increase in the total amount of carbon released under the assumption that all carbon stock in above ground biomass is released by deforestation. That is, we sum the carbon stock of all plots converted from forest to other uses in the counterfactual exercise. We estimate that the elasticity of carbon released with respect to crop prices is 0.11. This means, for example, that an increase of 10% in crop prices results in additional 0.5 billion tons of CO_2 release in steady state, amounting to $25 billion of costs if we consider a social cost of carbon of $50 per ton of CO_2 (EPA, 2016).

Table 6 Panel B reports land use elasticities with respect to cattle prices. We estimate a positive own land use price elasticity (column 3), but smaller than the cropland own price elasticity. Although we observe conversion of cropland to pastureland (cross elasticity of cropland with respect to cattle prices of -0.45), the main change in land use is the conversion of forest to pasture. We estimate a cross elasticity of forest cover with respect to crop land of -1.64, and a cross elasticity of carbon released of 1.66, substantially larger than the cross elasticities with respect to crop prices. This suggests that changes in the market conditions of cattle have greater impact on the forest than similar changes in annual crops markets. We return to this point when we discuss market policies to conserve the forest.

5.2 Efficient forestation

The socially optimal forest cover in the Amazon is the one in which agents fully internalize the externalities associated with deforestation when making land use choices. In our main

counterfactual exercise, we quantify the Amazon's efficient forestation in the steady state when agents internalize the social cost of carbon stored in each plot of forest. To do this, we equate agents' private perceived value of the carbon stored in the forest to the social cost of carbon released to the atmosphere. We use the value of social cost of carbon of \$50.00 per ton of CO_2 calculated by EPA (2016) for the year 2030 – we consider 2030 because our counterfactual computes the steady state land use, rather than the current short-run land use.

We calculate that the efficient forestation under a social cost of carbon of \$50/ton would imply an additional 1,075,000 km^2 in forest cover and 44 billion tons less of CO2 released into the atmosphere.[18] Remember that our sample include pixels outside protected areas which were not deforested prior 2000. We find that the efficient forest cover encompasses 90.77% of this area and that about 99.5% of the carbon stored in it should be preserved – in the business as usual steady state, we see only 47% of the stock of carbon preserved.

We further use the spatial granularity of the data to map the pixels that are likely to be inefficiently deforested in the status quo (i.e., the business as usual scenario). Figure (5) shows the difference of steady-state probabilities that each pixel is forested in the efficient and in the status-quo steady state. Lighter areas mark pixels that are more likely to be forested in the efficient scenario and are less likely to be forested in the status quo scenario. We see that in some areas efficient forestation implies an 80% higher probability of forest cover compared to the status quo, especially in areas around main waterways and roads in the state of Pará. This is mainly a combination of high carbon density (which drives up efficient forestation) and low transportation costs (which drives down forestation in status quo). Meanwhile, darker regions represent places in which the status quo is closer to efficiency. Those are areas very deep in the forest (far west), in which even though carbon stock is high, transportation costs are prohibitive, and areas with small carbon stock (on the Amazonian fringe) in the states of Mato Grosso and Tocantins.

We can benchmark these magnitudes relative to the deforestation process over the last twenty years. Hansen et al. (2013) shows that around 565,343 km^2 was deforested in Brazil between 2001 and 2019. De Azevedo et al. (2018) calculates that land use change in Brazil in this period released 20 billion tons of CO2. Thus, achieving the additional 1 million km^2 of forest cover and preserving 44 billion tons of CO2 in the efficient steady state means ceasing current deforestation pattern for the next four decades. Alternatively, it means regenerating most of the deforestation that took place over the last twenty years and stopping deforestation for the next twenty years. In sum, implementing the first-best forestation is a Herculean task.

[18] We compute the total area and carbon released by multiplying the steady-state probability of each pixel being forest by the pixel area (or carbon content), and summing all pixels in our sample.

Figure 5: Efficient forest cover relative to status quo

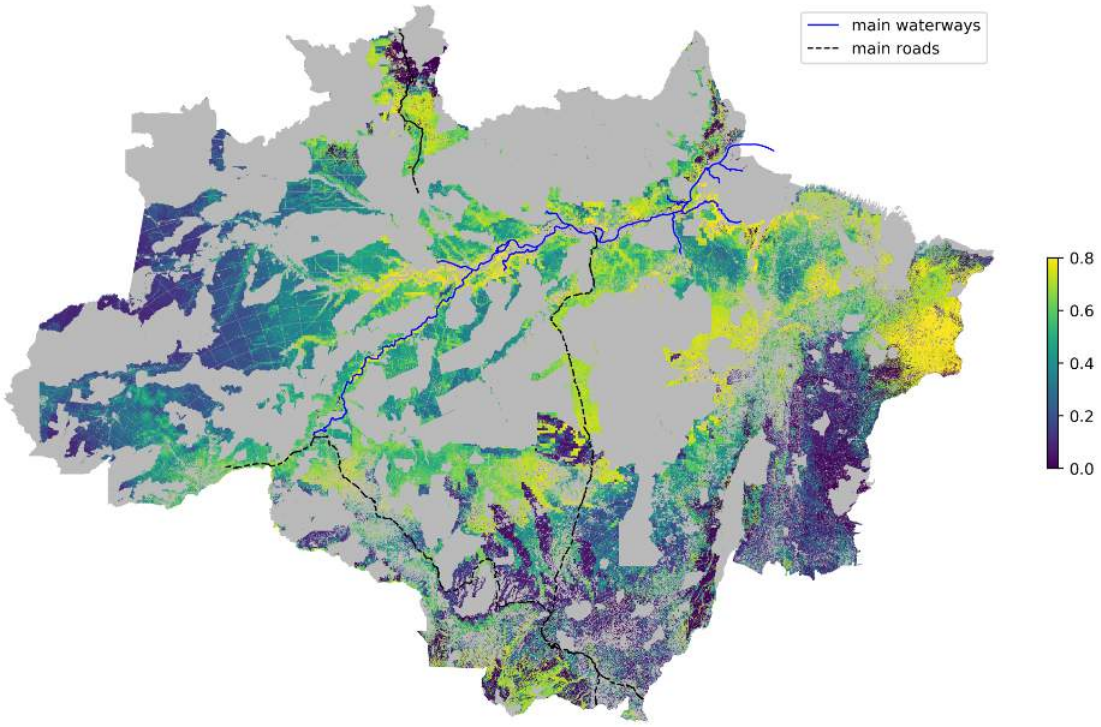

This figure shows the map with the difference of steady state probabilities of forest cover when agents fully internalize the marginal social costs of carbon – with perceived value of carbon $50 – and the status quo steady state – with perceived value of carbon $7.26.

In the rest of this section, we show how policies can help us to get closer to this efficient forestation.

5.3 Preserving the forest through carbon tax

We now consider how a carbon tax based on the carbon content of the land could shape farmers' incentives to use the land and promote forest conservation. As we discussed in the previous section, we interpret the estimate of the private return of carbon in the land as the perceived value of carbon as imposed by current conservation policies and enforcements. We ran counterfactual scenarios where we strengthen conservation policies by adding a carbon tax to be paid if the agent chooses to convert the forest to other use. Within our model, this is equivalent to providing a payment for ecosystem services (e.g., Alix-Garcia et al., 2015; Jayachandran et al., 2017; Wong et al., 2019) of the value of the carbon tax that is lost when the pixel is deforested. We can also interpret this carbon tax as an increase in the perceived value of carbon driven by stronger enforcement of environmental policies, such as using remote sensing data to detect deforestation (Assunção et al., 2017) and rural registries

to increase compliance (Alix-Garcia et al., 2018).[19]

Specifically, we calculate steady-state land use in different scenarios considering the inclusion of carbon taxes ranging from \$2.5/ton to \$20/ton. Table 7 reports results of additional forest cover (column 1) and CO2 released (column 2) in the steady state with carbon tax relative to the status quo. The main lesson this table shows us is that there is a strong non-linearity in the amount of forest preserved implied by carbon taxes, with relatively small carbon taxes closing a substantial share of the gap between the status quo and the efficient forestation. For example, a carbon tax of \$2.5/ton would preserve 306 thousand km^2 and 15 billion tons of CO_2, leading the forest 34% [=15/44] closer to its efficient forestation. In the steady state, a carbon tax of \$10/ton would preserve 84% [=37/44] of the efficient carbon stock. This non-linearity is intuitive: it is relatively cheaper to preserve carbon deeper in the forest, as carbon stock and transportation costs are higher there. As the marginal land being preserved comes closer to the agricultural frontier (lower carbon stock and transportation costs), it becomes increasingly costly to preserve carbon.

Table 7: Efficient forestation and counterfactual carbon tax

Carbon tax	Δ Forest cover $(1,000km^2)$	Δ CO_2 released (billion tons)
(1)	(2)	(3)
\$2.5	306	-15
\$5.0	540	-26
\$10.0	799	-37
\$20.0	977	-42

This table presents counterfactual results for the increase in forested area and decrease in emissions for different values of carbon taxes imposed on agents. Our baseline perceived carbon value implied by the model estimates is \$7.26 per ton of CO_2. Here, we consider smaller values of carbon tax – \$2.50, \$5.00, \$10.00, and \$20.00 – added to the baseline perceived value of carbon. The column Δ Forest cover gives the difference of steady-state forest cover between the baseline scenario and the alternative scenario. The ΔCO_2 released column gives total the difference of CO_2 released between the baseline and the alternative steady state scenario for all pixels we consider in our sample.

We can see the convexity in agents response to carbon taxes in Figure 6. The figure on the left shows the amount of forest cover under different carbon taxes, and the figure on the right shows the amount of carbon released in these different scenarios. In both cases, we consider carbon taxes up to \$42.74/ton, the value that implements the efficient forestation. Both graphs show a clear convexity, with most of the conservation gains being achieved with carbon taxes under \$20/ton. Above this point, additional reductions in carbon emissions

[19]See Burgess et al. (2019) for a complete set of policies implemented in the Amazon in this period.

Figure 6: Forest cover and carbon released by carbon taxes

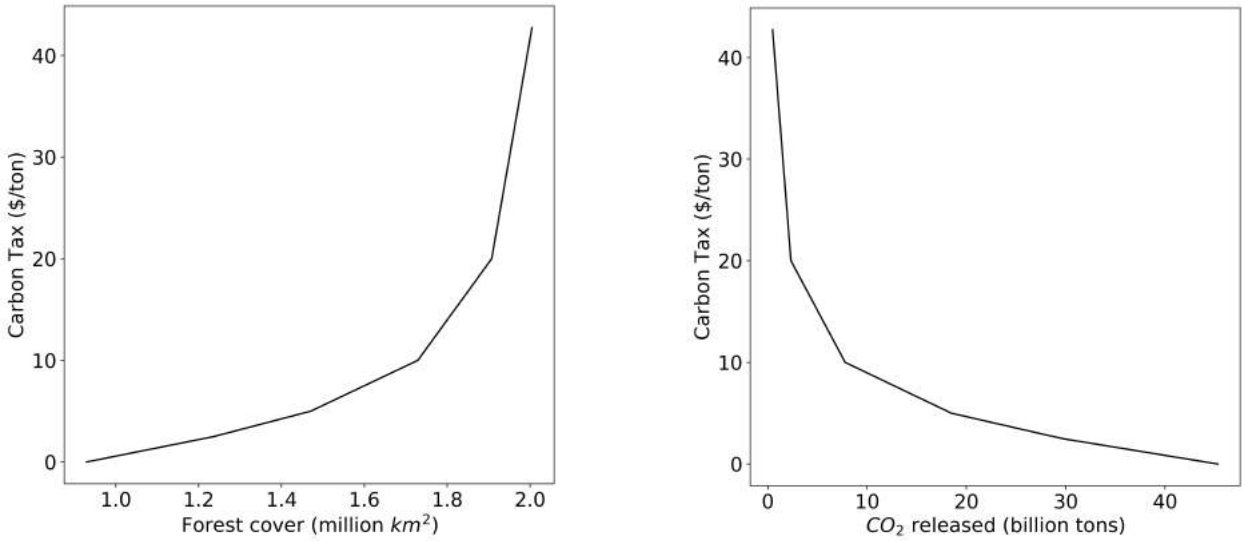

(a) Forest cover (km^2)

(b) Carbon emission (tons of CO_2)

These graphs display the steady state forest cover (a) and carbon released (b) for different carbon tax values.

become increasingly costly. This is in line with the estimates of Souza-Rodrigues (2019) that find that a carbon tax of $18.50/ton would make farmers in the Amazon indifferent between producing or preserving the forest.

5.4 Preserving the forest through taxes on cattle ranching

We now assess the potential effects of excise taxes on cattle ranching and crops to promote forest conservation. There are increasing discussions on how market interventions, such as international tariffs (Abman and Lundberg, 2020) or bans on goods produced in areas under deforestation pressure (e.g., Nepstad et al., 2014; Gibbs et al., 2015; Harding et al., 2019). We therefore compute the steady state land use under scenarios where agents are subject to taxes on cattle or on crop goods – i.e. an *ad valorem* tax on their final product. We evaluate, for each tax level between 0 to 100%, resulting emissions and forest cover.

Figure 7 displays the results. We find that the relationship between cattle taxes and forest cover and carbon released are also convex, however not as convex as carbon taxes. Figure 7b shows the amount of long-run carbon emissions for each level of tax on cattle ranching. Relatively smaller taxes, such as a 20% rate, can save about 16 billion tons of CO_2.[20] We find, however, that only substantially larger excise taxes can generate the same

[20]Note that we only consider emissions from the carbon released by deforestation, not the methane pro-

Figure 7: Effects of a cattle tax on forest cover and carbon released

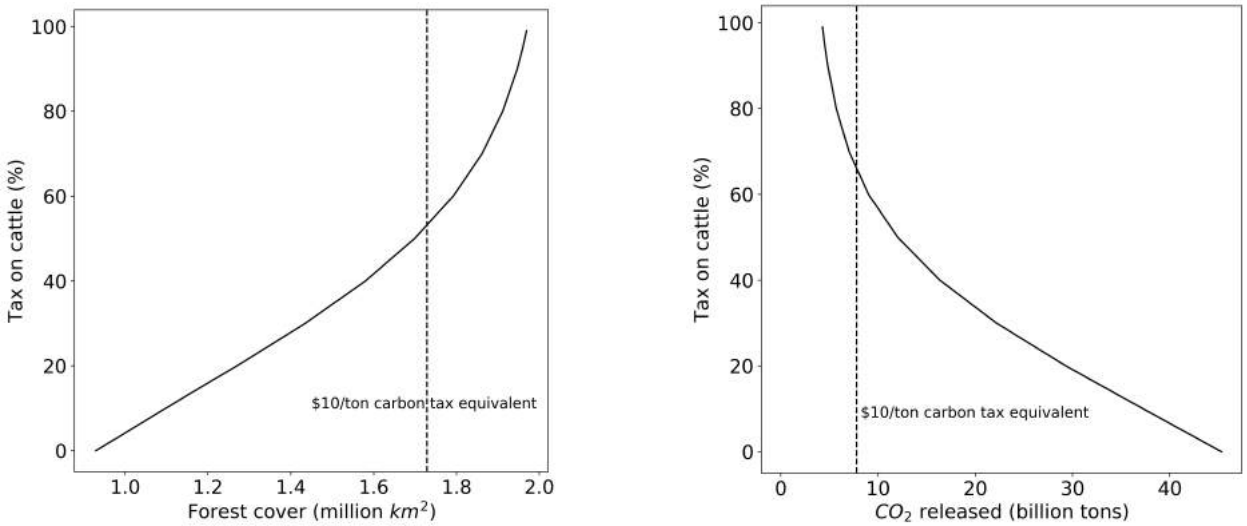

(a) Forest cover (km^2)

(b) Carbon emission (tons of CO_2)

Forest cover (a) and carbon emissions from deforestation (b) for different levels of excise taxes on cattle ranching. Dashed lines highlight forest cover (a) and carbon emissions (b) that would follow from a $10/ton carbon tax for comparison across policy exercises.

conservation as carbon taxes. For example, a 65% tax on cattle is necessary to save the same level of carbon as a $10/ton carbon tax – marked with a vertical dashed line in the figure. We see a similar pattern in Figure 7a that displays the amount of forest cover for each level of cattle tax. It shows that a 53% tax on cattle induces the same extent of forest cover in the steady state as the one implied by the $10/ton carbon tax. This difference in taxes arises from the fact that carbon stock is correlated with pasture suitability. We experimented with a tax on crops as well, but we found that the tax on crops produced only marginal relative changes in carbon emissions.

In sum, the low productivity economic activities currently in place in the region and the large amounts of carbon stored in the forest make a relatively small strengthening of environmental policies (i.e. small carbon taxes) go a long way in bringing the forest cover closer to the efficient forestation. On the other hand, current small opportunity costs of preserving the forest make almost any return from deforestation, such as converting to cattle ranching, economically attractive for agents. Thus, only really large excise taxes can disincentivize land use to the extent needed to mitigate inefficient carbon emissions from deforestation. If the objective is conserving forest acreage irrespective of carbon stock, taxes on cattle can be

duced by the cattle.

an effective tool to increase forest cover in the long-run.

6 Caveats and extensions

Our analysis relied on several assumptions and simplifications that may impact our conclusions. In this section, we discuss the main caveats that should help interpreting the results and present some extensions.

Loss in biodiversity and other externalities. We only look at carbon emissions when computing the social cost of deforestation. This ignores the potentially big externalities involved in the loss of biodiversity that follows deforestation. Moreover, we do not consider other externalities from the loss of green cover such as changes in rain patterns due to the disruption of water cycles (Malhi et al., 2008). These unmodelled effects are potentially big, but we know of no study explicitly computing social costs arising from these effects that we could directly apply to our setting. Therefore, we decided for the conservative approach of only factoring in social costs related to the release of carbon stored in the forest. However, we conjecture that these other externalities we cannot account for are all negative, making the optimal forest gap even larger once those are explicitly factored in.

Technology. We look at the steady state equilibrium choices under the current technologies used in agriculture and cattle ranching in the Amazon. It is plausible to imagine that farmers and ranchers in the region will slowly adopt more productive technologies over time such that, in the long run, the returns of agriculture will be higher. To assess how this issue could change our main results, we estimate an extension of the model where we model the return of agriculture using the most productive technology available in nearby regions in Brazil. Specifically, we consider that every pixel produces crop with a double crop system, producing soybeans in the main season and maize for the second season in the same agriculture year, and where soil suitability uses high inputs (see, e.g., Bustos et al., 2016).

Column 1 in Tables A3 and A4 show the estimates with double cropping. In this setting, we estimate a perceived value of carbon of \$ 16.29/ton of CO_2. This is larger than our baseline estimates because rationalizing the amount of forest seen in the data with a higher crop return, requires a higher forest return. Nonetheless, this perceived value of carbon is still substantially smaller than the social cost of carbon.

We estimate that that forest cover would be 874,000 km^2 larger in the efficient steady state than in the status quo, preventing 37 billion ton of CO_2 of being released to the atmosphere.

Table A5 Panel A shows the counterfactual forest cover and CO_2 released under the different carbon taxes. We still see a convex relationship between carbon price and emissions, but slightly less than in our main estimates in Table 7. For example, a \$10/ton carbon tax saves 67.6% of the efficient carbon emissions in the steady state with double crop, while it saves 74% in our main estimates.

Equilibrium effects. In our analysis we ignore possible equilibrium effects from the policies considered. This is valid if agricultural commodities here are internationally traded and this region represents a small share of the supply,[21] being insufficient to affect world prices. However, if this condition is not valid, an efficient carbon tax on deforestation or a tax on beef would decrease the supply of these commodities and push world prices up. This price increase could partially offset the decrease in deforestation by increasing acreage as we move to a new market equilibrium, as well as harming consumers worldwide. We note that this acreage increase would happen everywhere in the world, and not just in the Brazilian Amazon, which limits the severity of this simplification for our analysis.

Counterfactual simulations. There are a few caveats in our counterfactual simulations that merit some scrutiny. First, when we compute the long-run steady state we abstract from uncertainty in commodity prices and other market variables. The estimation method we employ allows us to be agnostic with respect to how farmers perceived transitions for those state variables. Therefore, to incorporate uncertainty in counterfactual simulations would require us to make additional assumptions and empirical work. This simplification also challenges the interpretation we could derive from transitions to the long run. For this reason, we also limited ourselves to comparing steady-states. Nonetheless, we believe that our exercise captures the main long run trade-offs between production and preservation.

7 Conclusion

In this paper we estimated the efficient level of carbon stored in the Brazilian Amazon forest using an original dynamic discrete choice model where farmers make decisions on land use. We used the estimated model to compute the long-run gap between the optimal forest and the one we will have under status quo practices and policies in the region. We find that such a gap is large as farmers currently value the carbon stored in the forest at \$7.26 per ton of

[21] In 2018, Brazil accounted for 10% of global cattle production, 7% of global maize and 34% of global soybeans (FAOSTAT).

CO_2, that is substantially smaller than current estimates of the social cost of carbon released to the atmosphere (EPA, 2016, e.g., estimates a social cost of carbon in 2030 of $50.00/ton).

We also used the model to quantify how the introduction of a carbon tax to land use or excise taxes on cattle ranching and crops can help closing, at least partially, such gap. We find a very non-linear response of forest cover to carbon taxes, such that relatively small carbon taxes can mitigate a substantial part of inefficient forest loss. Our counterfactuals also show that while crop taxes have virtually no effect on forestation, large taxes on cattle raised in the Amazon can be effective to partially close the efficiency gap.

Our results highlight the stark change in economic incentives needed to mitigate inefficient emissions from land use in the Amazon. While the logistics of implementing such policies are not simple, we understand that Brazil has demonstrated that it can use technology to enforce environmental compliance and that there is will from the international community to help fund it. On market side policies, we find that disincentivizing the main driver of deforestation in the region, cattle grazing, can also be effectively used to reduce inefficient forestation in the long run. Technologies such as cattle tracing and a moratorium on Amazonian beef are feasible options in this direction. Disincentivizing crop production in the region, on the other hand, does not look like such a promising alternative.

As with any research paper, ours has some limitations imposed by model assumptions and the data. We discussed caveats related to technology adoption and equilibrium considerations in the last section. We also highlight that we cannot account for the value of lost biodiversity caused by deforestation, so the optimal forest gap we estimate should be seen as a lower bound. Nevertheless, we believe the numbers provided in this paper make a sensible contribution by quantifying how the current land use pattern in the Amazon is driving the region very far away from its long run efficient forestation, and informing the policy debate surrounding mitigation of carbon emissions from land use change in the Amazon.

References

Abman, R. and Lundberg, C. (2020). Does Free Trade Increase Deforestation? The Effects of Regional Trade Agreements. *Journal of the Association of Environmental and Resource Economists*, 7(1):35–72.

Aguirregabiria, V. and Mira, P. (2007). Sequential Estimation of Dynamic Discrete Games. *Econometrica*, 75(1):1–53.

Alix-Garcia, J., Rausch, L. L., L'Roe, J., Gibbs, H. K., and Munger, J. (2018). Avoided Deforestation Linked to Environmental Registration of Properties in the Brazilian Amazon. *Conservation Letters*, 11(3):e12414.

Alix-Garcia, J. M., Sims, K. R., and Yañez-Pagans, P. (2015). Only One Tree from Each Seed? Environmental Effectiveness and Poverty Alleviation in Mexico's Payments for Ecosystem Services Program. *American Economic Journal: Economic Policy*, 7(4):1–40.

Anderson, T. W. and Hsiao, C. (1981). Estimation of Dynamic Models with Error Components. *Journal of the American Statistical Association*, 76(375):598–606.

Arellano, M. and Bond, S. (1991). Some Tests of Specification for Panel Data: Monte Carlo Evidence and an Application to Employment Equations. *Review of Economic Studies*, 58(2):277–297.

Asher, S., Garg, T., and Novosad, P. (2020). The Ecological Impact Of Transportation Infrastructure. *Economic Journal*. ueaa013.

Assunção, J., Gandour, C., and Rocha, R. (2017). DETERring Deforestation in the Brazilian Amazon: Environmental Monitoring and Law Enforcement. Technical report, available at https://www.climatepolicyinitiative.org/publication/deterring-deforestation-in-the-brazilian-amazon-environmental-monitoring-and-law-enforcement/.

Assunção, J., McMillan, R., Murphy, J., and Souza-Rodrigues, E. (2019). Optimal Environmental Targeting in the Amazon Rainforest. Technical report, National Bureau of Economic Research.

Assunção, J., Costa, F., and Szerman, D. (2020). Environmental Regulation and Political Interference: Evidence from Power Plants in the Amazon. Technical report, working paper.

Assunção, J., Gandour, C., and Rocha, R. (2015). Deforestation Slowdown in the Brazilian Amazon: Prices or Policies? *Environment and Development Economics*, 20(6):697–722.

Baccini, A., Goetz, S. J., Walker, W., Laporte, N. T., Sun, M., Sulla-Menashe, D., Hackler, J., Beck, P., Dubayah, R., Friedl, M., Samanta, S., and Houghton., R. A. (2012). Estimated Carbon Dioxide Emissions from Tropical Deforestation Improved by Carbon-Density Maps. *Nature Climate Change*.

Bastin, J.-F., Finegold, Y., Garcia, C., Mollicone, D., Rezende, M., Routh, D., Zohner, C. M., and Crowther, T. W. (2019). The Global Tree Restoration Potential. *Science*, 365(6448):76–79.

Burgess, R., Costa, F., and Olken, B. (2019). The Brazilian Amazon's Double Reversal of Fortune. Technical report, working paper.

Bustos, P., Caprettini, B., and Ponticelli, J. (2016). Agricultural Productivity and Structural Transformation: Evidence from Brazil. *American Economic Review*, 106(6):1320–65.

Chomitz, K. and Gray, D. A. (1999). *Roads, Lands, Markets, and Deforestation: A Spatial Model of Land Use in Belize*. The World Bank.

Costinot, A., Donaldson, D., and Smith, C. (2016). Evolving Comparative Advantage and the Impact of Climate Change in Agricultural Markets: Evidence from 1.7 Million Fields Around the World. *Journal of Political Economy*, 124(1):205–248.

De Azevedo, T. R., Junior, C. C., Junior, A. B., dos Santos Cremer, M., Piatto, M., Tsai, D. S., Barreto, P., Martins, H., Sales, M., Galuchi, T., et al. (2018). SEEG Initiative Estimates of Brazilian Greenhouse Gas Emissions from 1970 to 2015. *Scientific Data*, 5:180045.

Donaldson, D. (2018). Railroads to Raj. *American Economic Review*, 108(4-5):899–934.

Donaldson, D. and Hornbeck, R. (2016). Railroads and American Economic Growth: A "Market Access" Approach. *Quarterly Journal of Economics*, 131(2):799–858.

EPA (2016). Social Cost of Carbon. *Environmental Protection Agency (EPA): Washington, DC, USA*.

Fezzi, C. and Bateman, I. J. (2011). Structural Agricultural Land Use Modeling for Spatial Agro-Environmental Policy Analysis. *American Journal of Agricultural Economics*, 93(4):1168–1188.

Friedlingstein, P., Jones, M., O'sullivan, M., Andrew, R., Hauck, J., Peters, G., Peters, W., Pongratz, J., Sitch, S., Le Quéré, C., et al. (2019). Global Carbon Budget. *Earth System Science Data*, 11(4):1783–1838.

Gibbs, H. K., Rausch, L., Munger, J., Schelly, I., and Morton, D. C. e. a. (2015). Brazil's Soy Moratorium. *Science*, 347(6220):377–378.

Hansen, M. C., Potapov, P. V., Moore, R., Hancher, M., Turubanova, S., Tyukavina, A., Thau, D., Stehman, S., Goetz, S., Loveland, T., et al. (2013). High-Resolution Global Maps of 21st-Century Forest Cover Change (v1.6). *Science*, 342(6160):50–853.

Harding, T., Herzberg, J., and Kuralbayeva, K. (2019). Commodity Prices and Robust Environmental Regulation: Evidence from Deforestation in Brazil. Technical report, working paper.

Heilmayr, R., Echeverría, C., and Lambin, E. F. (2020). Impacts of Chilean Forest Subsidies on Forest Cover, Carbon and Biodiversity. *Nature Sustainability*, 3(9):701–709.

Hornbeck, R. (2010). Barbed Wire: Property Rights and Agricultural Development. *Quarterly Journal of Economics*, 125(2):767–810.

Hotz, V. J. and Miller, R. A. (1993). Conditional Choice Probabilities and the Estimation of Dynamic Models. *Review of Economic Studies*, 60(3):497–529.

IPCC (2007). *Climate Change 2007: Synthesis Report. Contribution of Working Groups I, II and III to the Fourth Assessment Report of the Intergovernmental Panel on Climate Change*. Geneva, Switzerland.

IPCC (2019). 2019 Refinement to the 2006 IPCC Guidelines for National Greenhouse Gas Inventories. Volume 4 Agriculture, Forestry and Other Land Use. Calvo Buendia, E., Tanabe, K., Kranjc, A., Baasansuren, J., Fukuda, M., Ngarize S., Osako, A., Pyrozhenko, Y., Shermanau, P. and Federici, S. (eds). *Published: IPCC, Switzerland.*

Jayachandran, S., De Laat, J., Lambin, E. F., Stanton, C. Y., Audy, R., and Thomas, N. E. (2017). Cash for Carbon: A Randomized Trial of Payments for Ecosystem Services to Reduce Deforestation. *Science*, 357(6348):267–273.

Lubowski, R. N., Plantinga, A. J., and Stavins, R. N. (2006). Land-use Change and Carbon Sinks: Econometric Estimation of the Carbon Sequestration Supply Function. *Journal of Environmental Economics and Management*, 51(2):135–152.

Lubowski, R. N., Plantinga, A. J., and Stavins, R. N. (2008). What Drives Land-Use Change in the United States? A National Analysis of Landowner Decisions. *Land Economics*, 84(4):529–550.

Malhi, Y., Roberts, J. T., Betts, R. A., Killeen, T. J., Li, W., and Nobre, C. A. (2008). Climate Change, Deforestation, and the Fate of the Amazon. *Science*, 319(5860):169–172.

MapBiomas, P. (2019). Collection4.0.

Nepstad, D., McGrath, D., Stickler, C., Alencar, A., Azevedo, A., Swette, B., Bezerra, T., DiGiano, M., Shimada, J., da Motta, R. S., et al. (2014). Slowing Amazon Deforestation Through Public Policy and Interventions in Beef and Soy Supply Chains. *Science*, 344(6188):1118–1123.

Nordhaus, W. (2014). Estimates of the Social Cost of Carbon: Concepts and Results from the DICE-2013R Model and Alternative Approaches. *Journal of the Association of Environmental and Resource Economists*, 1(1/2):273–312.

Pattanayak, S. K., Wunder, S., and Ferraro, P. J. (2010). Show Me the Money: Do Payments Supply Environmental Services in Developing Countries? *Review of Environmental Economics and Policy*, 4(2):254–274.

Pellegrina, H. (2020). Trade, Productivity, and the Spatial Organization of Agriculture: Evidence from Brazil. Technical report, working paper.

Rosen, S., Murphy, K. M., and Scheinkman, J. A. (1994). Cattle Cycles. *Journal of Political Economy*, 102(3):468–492.

Sant'Anna, M. (2020). How Green is Sugarcane Ethanol? *working paper*.

Scott, P. (2018). Dynamic Discrete Choice Estimation of Agricultural Land Use. *working paper*.

Souza-Rodrigues, E. (2019). Deforestation in the Amazon: A Unified Framework for Estimation and Policy Analysis. *Review of Economic Studies*, 86(6):2713–2744.

Wong, P. Y., Harding, T., Kuralbayeva, K., Anderson, L. O., and Pessoa, A. M. (2019). Pay for Performance and Deforestation: Evidence from Brazil. Technical report, working paper.

A Appendix Model

Here we provide more details on the derivation of the regression equation. The steps below follow closely in spirit the derivation in Scott (2018). From (3) and (6), we have:

$$\Phi(j,k) + r_m(j,w_t) - \Phi(j',k) - r_m(j',w_t) - \log\left(\frac{p_m(j|k,w_t)}{p_m(j'|k,w_t)}\right) = \\ \rho E\left[\bar{V}_m(j',w_{t+1})|w_t\right] - \rho E\left[\bar{V}_m(j,w_{t+1})|w_t\right], \text{ for } k,j,j' \in J. \quad (19)$$

Let $\eta_m^V(j,w_t) := \rho(E\left[\bar{V}_m(j,w_{t+1})|w_t\right] - \bar{V}_m(j,w_{t+1}))$ denote the expectation error in continuation values. We can re-write (19) as

$$\Phi(j,k) + r_m(j,w_t) - \Phi(j',k) - r_m(j',w_t) - \log\left(\frac{p_m(j|k,w_t)}{p_m(j'|k,w_t)}\right) = \\ \rho(\bar{V}_m(j',w_{t+1}) - \bar{V}_m(j,w_{t+1})) + \eta_m^V(j',w_t) - \eta_m^V(j,w_t), \text{ for } k,j,j' \in J. \quad (20)$$

Another implication of the logit errors assumption is that $\bar{V}_m(j',w_t)$ has a convenient expression:

$$\bar{V}_m(k,w_t) = \log\left(\sum_{j\in J}\exp\left(v_m(j,k,w_t)\right)\right) + \gamma, \text{ for all } k \in J, \quad (21)$$

where γ is the Euler's gamma. From (6) and (21), for all $k \in J$, we can write

$$\bar{V}_m(k,w_t) = v_m(l,k,w_t) - \log\left(p_m(l|k,w_t)\right) + \gamma, \text{ for all } l \in J. \quad (22)$$

We use the representation in (22) to cancel common continuation terms in the difference $\bar{V}_m(j',w_{t+1}) - \bar{V}_m(j,w_{t+1})$ in (20). Replacing (22) in (20), we have

$$\Phi(j,k) + r_m(j,w_t) - \Phi(j',k) - r_m(j',w_t) - \log\left(\frac{p_m(j|k,w_t)}{p_m(j'|k,w_t)}\right) = \\ \rho(v_m(l,j',w_{t+1}) - v_m(l,j,w_{t+1})) - \rho\log\left(\frac{p_m(l|j',w_{t+1})}{p_m(l|j,w_{t+1})}\right) + \\ \eta_m^V(j',w_t) - \eta_m^V(j,w_t), \text{ for } l,k,j,j' \in J. \quad (23)$$

From the definition of $v_m(\cdot)$, $v_m(l,j',w_{t+1}) - v_m(l,j,w_{t+1}) = \Phi(l,j') - \Phi(l,j)$. That is, all

continuation terms cancel out and we can simplify further (20):

$$\Phi(j,k) + r_m(j,w_t) - \Phi(j',k) - r_m(j',w_t) - \log\left(\frac{p_m(j|k,w_t)}{p_m(j'|k,w_t)}\right) = \rho(\Phi(l,j') - \Phi(l,j)) - \rho\log\left(\frac{p_m(l|j',w_{t+1})}{p_m(l|j,w_{t+1})}\right) + \eta_m^V(j',w_t) - \eta_m^V(j,w_t), \text{ for } l,k,j,j' \in J. \quad (24)$$

Using assumption 3, for $l = j$ and $k = j'$, we can re-write (24) as

$$\log\left(\frac{p_m(j|k,w_t)}{p_m(k|k,w_t)}\right) - \rho\log\left(\frac{p_m(j|k,w_{t+1})}{p_m(j|j,w_{t+1})}\right) = (1-\rho)\Phi(j,k) + r_m(j,w_t) - r_m(k,w_t) + \eta_m^V(j,w_t) - \eta_m^V(k,w_t), \text{ for } j,k \in J. \quad (25)$$

We delay until the next subsection an exact specification for $r_m(\cdot)$. For now, it is important to note that it assumes a linear formulation in unknown parameters with an unobservable (to the econometrician) component:

$$r_m(j,w_t) = \bar{\alpha}_j + \alpha_j' R_j(x_m,w_t) + \xi_{jm}(w_t), \quad (26)$$

where $R_j(x_m,w_t)$ are observed regressors and $\bar{\alpha}_j$ is an intercept.

B Appendix Figures and Tables

Figure A1: Federal and state roads networks

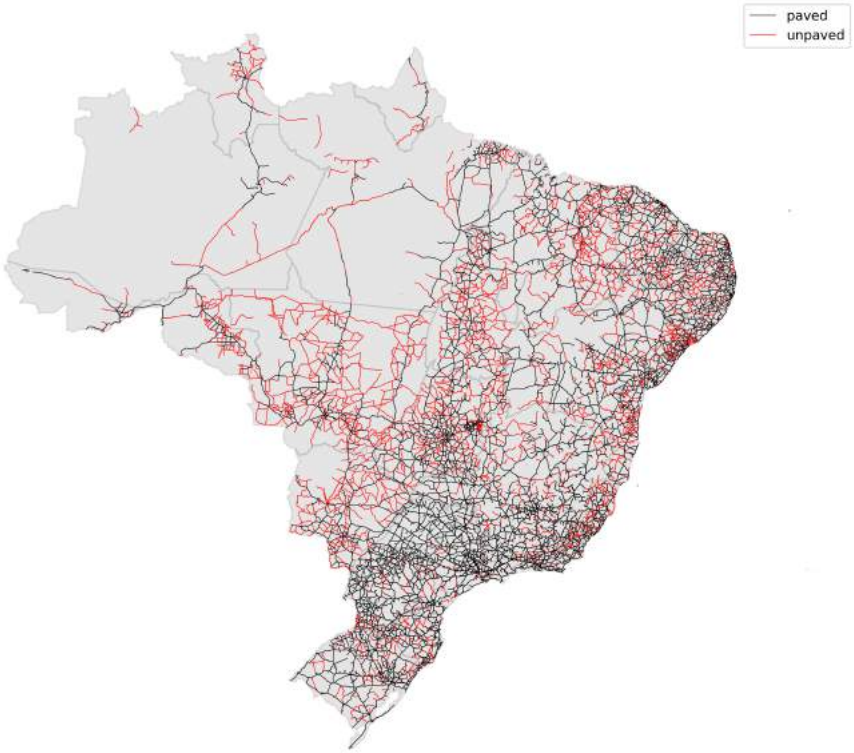

This map shows the state and federal road networks we use to compute transportation costs. Black lines show paved roads and red lines show unpaved roads.

Figure A2: Pairs of origin/destination freight costs from ESALQ

Each black line in the map represents an origin/destination pair in the ESALQ freight costs dataset.

Table A1: Estimates to monetize transportation cost

	Soybeans	Maize
	(1)	(2)
Coefficient (β_1)	0.0723	0.0713
	(0.001)	(0.001)
Constant ($= \beta_0$)	5.3169	7.789
	(1.341)	(1.410)
R^2	0.844	0.883
N. obs	1200	972

This table presents the estimates of the non-linear least squares regressions from equation (15).

Figure A3: Ports and waterways transportation costs

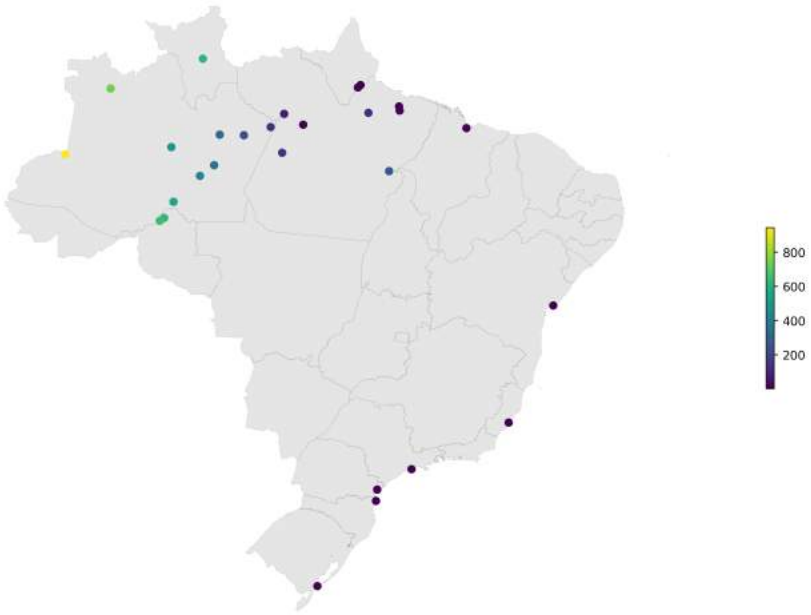

This map shows the waterways and the main ports in the Amazon we consider to estimate transportation cost. The colors in the dots show how much it costs to reach the closer final port – i.e., ports with direct access to international markets. Ports with zero cost are final ports.

Table A2: Crop flow profit coefficient

Regressor	Estimate (1)	Estimate (2)
$\tilde{r}_{i,t-2}$	0.04322***	0.04605***
	(2.19e-5)	(1.78e-5)
$W_{j,k,i,2011}$	-3.27e-2***	-4.78e-2***
	(1.60e-5)	(2.64e-5)
$W_{j,k,i,2012}$	-7.66e-4***	-3.46e-2***
	(1.59e-5)	(2.63e-5)
$W_{j,k,i,2013}$	2.90e-2***	5.38e-2***
	(1.61e-5)	(2.65e-5)
$W_{j,k,i,2014}$	1.76e-2***	4.02e-2***
	(1.61e-5)	(2.66e-5)
$W_{j,k,i,2015}$	1.03e-2***	2.58e-2***
	(1.60e-5)	(2.65e-5)
$W_{j,k,i,2016}$	-4.30e-2***	-6.06e-2***
	(1.60e-5)	(2.64e-5)

This table presents the first stage estimates using the lagged values $\tilde{r}_{i,t-2}$ as an instrument for $X_{j,k,i,t}$. The first column reports regressors. Robust standard errors in parenthesis. Number of observations 79,473,168.Estimate (1) shows the results when the crop revenue net of transportation cost is a weighted average of soy and naize, where the weights are the proportion of the product in the region that the pixels lies inside. Estimate(2) shows the result when we consider that every pixel will apply a double crop system, producing soy and maize of second season in the same year. F statistics for specification (1) is 3,107,226. F statistics for specification (2) is 3,796,531

Table A3: Extensions – Crop flow profit coefficient

Regressor	Model Parameter	Estimate (2)
$X_{j,k,m,t}$	α_{crop}	0.00021***
		(7.91e-7)
$W_{j,k,m,2011}$	$\Delta\alpha^1_{pasture,2011}$	3.30e-5***
		(6.98e-8)
$W_{j,k,m,2012}$	$\Delta\alpha^1_{pasture,2012}$	-2.30e-6***
		(5.49e-8)
$W_{j,k,m,2013}$	$\Delta\alpha^1_{pasture,2013}$	-4.00e-5***
		(6.28e-8)
$W_{j,k,m,2014}$	$\Delta\alpha^1_{pasture,2014}$	3.00e-5***
		(5.97e-8)
$W_{j,k,m,2015}$	$\Delta\alpha^1_{pasture,2015}$	-5.65e-5***
		(4.58e-8)
$W_{j,k,m,2016}$	$\Delta\alpha^1_{pasture,2016}$	5.59e-5***
		(7.18e-8)

This table shows the estimates of α_{crop} obtained in the second stage regression (equation 16) using Anderson and Hsiao (1981) estimator. Estimate (2) shows the result when we consider that every pixel will apply a double crop system, producing soy and maize of second season in the same year. The first column reports regressors, while the second column displays the corresponding model parameters from Section 2.2, equations (13) and (14). Robust standard errors in parenthesis. Number of observations 79,473,168.

Table A4: Extensions – Forest and pasture flow profits coefficients

Regressor	Model Parameter	Estimate (2)	$\backslash\alpha_{crop}$
h_m	α_{forest}	0.00073***	3.37
		(4.22e-7)	
$W_{j,k,m}$	$\alpha^1_{pasture,2011}$	7.52e-5***	-
		(3.60e-8)	
$W_{j,k,m}d_m$	$\alpha^2_{pasture}$	-7.02e-7***	-
		(1.91e-9)	
Fixed effects			
	$\Phi(pasture, forest)$	-6.23e-1***	-2896.18
		(1.58e-4)	
	$\Phi(crop, forest)$	-9.68e-1***	-4504.72
		(3.01e-4)	
	$\Phi(crop, pasture)$	-5.97e-1***	-2775.41
		(3.11e-4)	
	$\Phi(pasture, crop)$	-2.00e-1***	-931.03
		(3.07e-4)	
	$\bar{\alpha}_{pasture}$	1.57e-1***	731.46
		(1.84e-4)	
	$\bar{\alpha}_{crop}$	-6.50e-1***	-3022.61
		(2.55e-4)	

This table presents the OLS estimates of equation (9), using $\hat{\alpha}_{crop}$ and $\Delta\alpha^1_{pasture,t}$ estimated in equation (16) using Anderson and Hsiao (1981). Estimate (2) shows the result when we consider that every pixel will apply a double crop system, producing soy and maize of second season in the same year. The first column reports regressors, while the second column displays the corresponding model parameters from Section 2.2, equations (13) and (14). Robust standard errors in parenthesis. Number of observations 79,473,168.

Table A5: Extensions – Efficient forestation and counterfactual carbon tax

Carbon tax	Δ Forest cover $(1,000km^2)$	Δ CO_2 released (billion tons)
(1)	(2)	(3)
Panel A. Double cropping agriculture		
\$2.5	161	-8
\$5.0	304	-15
\$10.0	521	-25
\$20.0	750	-34
\$33.7	874	-37

This table presents counterfactual results for the increase in forested area and decrease in emissions for different values of carbon taxes imposed on agents for two model extensions. Panel A shows the result when we consider that every pixel will apply a double crop system, producing soy and maize of second season in the same year. Our baseline perceived carbon value implied by the model estimates is \$16.29 per ton of CO_2. Here, we consider smaller values of carbon tax – \$2.50, \$5.00, \$10.00, \$20.00, and \$33.70 – added to the baseline perceived value of carbon. The column Δ Forest cover gives the difference of steady-state forest cover between the baseline scenario and the alternative scenario. The $\Delta CO_2 released$ column gives total the difference of CO_2 steady-state released between the baseline and the alternative scenario for all pixels we consider in our sample.